INTERNATIONAL JOURNAL FOR NUMERICAL METHODS IN ENGINEERING
Int. J. Numer. Meth. Engng 2010; **84**:1407–1450
Published online 4 August 2010 in Wiley Online Library (wileyonlinelibrary.com). DOI: 10.1002/nme.2942

Force-stepping integrators in Lagrangian mechanics

M. Gonzalez[1], B. Schmidt[2] and M. Ortiz[1,*,†]

[1]*Graduate Aeronautical Laboratories, California Institute of Technology, Pasadena, CA 91125, U.S.A.*
[2]*Zentrum Mathematik, Technische Universität München, Boltzmannstr. 3, 85747 Garching, Germany*

SUMMARY

We formulate an integration scheme for Lagrangian mechanics, referred to as the *force-stepping scheme*, which is symplectic, energy conserving, time-reversible, and convergent with automatic selection of the time-step size. The scheme also conserves approximately all the momentum maps associated with the symmetries of the system. The exact conservation of momentum maps may additionally be achieved by recourse to the Lagrangian reduction. The force-stepping scheme is obtained by replacing the potential energy by a piecewise affine approximation over a simplicial grid or regular triangulation. By taking triangulations of diminishing size, an approximating sequence of energies is generated. The trajectories of the resulting approximate Lagrangians can be characterized explicitly and consist of piecewise parabolic motion, or *free fall*. Selected numerical tests demonstrate the excellent long-term behavior of force-stepping, its automatic time-step selection property, and the ease with which it deals with constraints, including contact problems. Copyright © 2010 John Wiley & Sons, Ltd.

Received 6 January 2010; Revised 1 April 2010; Accepted 17 April 2010

KEY WORDS: Lagrangian mechanics; time-integration; symplectic integrators; energy-momentum integrators

1. INTRODUCTION

In a recent paper [1], the authors have proposed a method of approximation for Lagrangian mechanics consisting of replacing the Lagrangian $L(q,\dot{q})$ of the system by a sequence of approximate Lagrangians $L_h(q,\dot{q})$ that can be *solved exactly*. The approximate solutions $q_h(t)$ are then the *exact* trajectories of $L_h(q,\dot{q})$. In this manner, the approximate solutions are themselves trajectories of a Lagrangian system and, therefore, have many of the properties of such trajectories such as symplecticity and exact energy conservation. If, in addition, the approximation of the Lagrangian preserves its symmetry group, then the approximate trajectories conserve all the momentum maps

*Correspondence to: M. Ortiz, Graduate Aeronautical Laboratories, California Institute of Technology, Pasadena, CA 91125, U.S.A.
†E-mail: ortiz@aero.caltech.edu

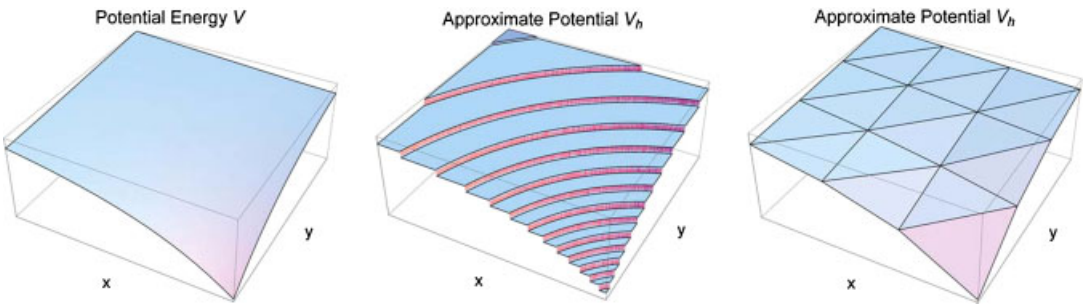

Figure 1. Kepler problem. Exact, piecewise constant and continuous piecewise-linear approximate potential energies.

of the system. It bears emphasis that, in contrast to variational integrators (cf. e.g. [2–4]), the momenta that are conserved are the exact momenta of the system and not some time discretization thereof. Finally, if the approximate Lagrangians $L_h(q,\dot{q})$ converge to the exact one $L(q,\dot{q})$ in a topology that implies, in particular, convergence of stationary points, then the approximate trajectories $q_h(t)$ converge to exact trajectories $q(t)$ of the original system.

In [1], this program has been carried out in full for Lagrangians of the type: $L(q,\dot{q})=K(\dot{q})-V(q)$, with $K(\dot{q})$ a quadratic form, and for approximate Lagrangians of the type $L_h(q,\dot{q})=K(\dot{q})-V_h(q)$, with $V_h(q)$ a terraced piecewise constant approximation to $V(q)$, Figure 1(b). This type of approximation does indeed result in exactly solvable Lagrangians. The approximate trajectories are piecewise rectilinear, with the intervals of rectilinear motion spanning consecutive level contours of the potential. Conveniently, the terraced potential $V_h(q)$ has all the symmetries of the original potential $V(q)$, and the approximate trajectories exactly conserve all the momentum maps of the system, whether explicitly known or otherwise. The durations of the intervals of rectilinear motion may be regarded as time steps, whose determination is part of the solution process. In this manner, the approach overcomes an intrinsic limitation of fixed time-step variational integrators, which cannot simultaneously conserve energy, the symplectic structure, and other conserved quantities, such as linear and angular momenta [5]. Under mild restrictions on the potential, the approximate trajectories are found to indeed converge to exact trajectories of the system, subject to technical transversality constraints.

The terraced piecewise constant approximation of the potential considered in [1] may be thought of as the lowest order approximation that results in convergence. Evidently, approximations of increasing order can be obtained by recourse to piecewise polynomial interpolation of the potential. In this paper, we consider the next order of approximation consisting of approximate potentials $V_h(q)$ obtained by piecewise-linear interpolation of $V(q)$ over structured simplicial meshes, Figure 1(c). Evidently, within each simplicial element in the interpolation mesh, the forces are constant, hence the term *force-stepping*, and the system is in *free fall*. In particular, the approximate Lagrangian can be solved exactly and the approximate trajectories are piecewise quadratic. In Section 3, we provide an efficient implementation of the scheme that establishes its feasibility in practical, possibly high dimensional, applications. In particular, we show in Section 6 that the typical numbers of time steps, or time intervals between crossings of simplicial boundaries, and their sizes are within the expected range for explicit integration. In Section 5, we show that the approximate trajectories thus computed do indeed converge to exact trajectories of the system.

DOI: 10.1002/nme

However, the matter of conservation requires careful attention as the piecewise-linear approximate Lagrangians break the symmetries of the system in general, which in turn results in a lack of exact momentum conservation of the force-stepping scheme. This symmetry breaking raises an interesting challenge which is not present in the case of the energy-stepping scheme and which we address in several ways. The first way to deal with the lack of exact conservation of the force-stepping scheme—and possibly the most effective—is to do nothing. Indeed, we show in Section 4 that the force-stepping scheme is nearly conserving for all symmetries of the system, whether explicitly known or otherwise. The conservation error is controlled uniformly on compact time intervals by the asymmetry of the approximate Lagrangian. The numerical experiments presented in Section 6 further show that the corresponding momentum maps tend to remain nearly uniformly constant for all times. This near-conservation property is frequently sufficient in applications that require good long-time behavior of the solutions. An alternative strategy, described in Section 4.2, for avoiding broken symmetries in the force-stepping scheme is to appeal to the theory of Lagrangian reduction. For symmetries for which explicit reduced Lagrangians are known, an application of the force-stepping scheme to the reduced Lagrangian results in exact momentum conservation. A case in point is translational invariance, which can be dealt with effectively by the introduction of Jacobi and center of mass coordinates.

The paper is organized as follows. The force-stepping time-integration scheme is defined in Section 2 and the construction of continuous piecewise-linear approximate energies is discussed in Section 3. The conservation properties of force-stepping, together with a general procedure for reducing translational symmetry, are presented in Section 4. In Section 5 we prove the convergence of trajectories except for a negligibly small set of initial conditions. In Section 6 we present selected example of application that illustrate the convergence, accuracy, and conservation properties of force-stepping, including the motion of two bodies which attract each other by Newton's law of gravitation, that is the Kepler problem, the dynamics of a frozen argon cluster, and the oblique impact of an elastic cube. Finally, a summary and concluding remarks are drawn in Section 7.

2. FORCE-STEPPING INTEGRATORS

For definiteness, we specifically consider dynamical systems characterized by Lagrangians $L: \mathbb{R}^d \times \mathbb{R}^d \to \mathbb{R}$ of the form

$$L(q, \dot{q}) = \tfrac{1}{2}\dot{q}^{\mathrm{T}} M \dot{q} - V(q), \tag{1}$$

where M is the mass matrix and V is the potential energy. Lagrangians of this form arise in a number of areas of application including structural dynamics, celestial mechanics, and molecular dynamics. The trajectories of a Lagrangian system can be approximated by replacing $L(q, \dot{q})$ by an approximating Lagrangian $L_h(q, \dot{q})$ that can be solved exactly. A particular type of approximating Lagrangian is

$$L_h(q, \dot{q}) = \tfrac{1}{2}\dot{q}^{\mathrm{T}} M \dot{q} - V_h(q) \tag{2}$$

obtained by introducing an approximation of the potential energy. In this work, we specifically investigate continuous piecewise-linear approximations of the potential energy. Thus, we construct a regular triangulation $\mathscr{T}_h$ of $\mathbb{R}^d$, as shown in Section 3, and define V_h as the corresponding continuous piecewise affine approximation of V. By taking triangulations of diminishing size, an approximating sequence of energies and Lagrangians is generated in this manner.

DOI: 10.1002/nme

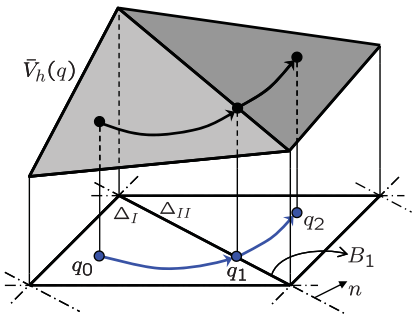

Figure 2. Trajectory of a system whose potential energy is approximated as continuous piecewise-linear.

The chief characteristics of the new systems thus obtained are that they can be solved exactly, as demonstrated in Section 2.1, and that they retain symmetries of the original system, as shown in Section 4. In contrast to piecewise constant interpolations of the potential energy, which preserve all the symmetries of the system [1], piecewise-linear interpolations break some symmetries in general. This difficulty can be partially overcome by recourse to Lagrangian reduction, as demonstrated in Section 4. However, we emphasize that the only assumption on the Lagrangian is its form—Equation (1)—and therefore no further considerations to Lagrangian reduction will be required in this section, i.e. $L(q,\dot{q})$ may also be a reduced Lagrangian.

Piecewise constant and piecewise-linear approximations of the Kepler potential are shown in Figure 1 by way of illustration.

2.1. Computation of the exact trajectories of the approximating Lagrangian

We now proceed to explicitly compute the exact trajectories of the approximate Lagrangian $L_h(q,\dot{q})$ resulting from V_h, the continuous piecewise-linear approximation of the potential energy. Suppose that the system is in configuration q_0 at time t_0 and in configuration q_2 at time t_2 and that during the time interval $[t_0,t_2]$ the system intersects one single boundary B_1 separating two regions Δ_I and Δ_{II}, of the underlying triangulation, with linear energies $V_I+\nabla V_I\cdot(q-q_I)$ and $V_{II}+\nabla V_{II}\cdot(q-q_{II})$, Figure 2. By the construction of V_h, the following continuity condition is attained at the boundary surface B_1

$$V_I+\nabla V_I\cdot(q-q_I)=V_{II}+\nabla V_{II}\cdot(q-q_{II})\quad\forall q\in B_1. \tag{3}$$

For simplicity, we shall further assume that V is differentiable and that all boundary crossings are transversal, i.e.

$$n(q_1)\cdot\dot{q}_1\neq 0, \tag{4}$$

where $n(q_1)$ is a vector normal to B_1 pointing in the direction of advance. It is possible for discrete trajectories to be non-transversal and therefore become ambiguously defined. However, the set of initial conditions that result in non-transversal trajectories has negligible dimension and will not be given further consideration. More precisely, we will show in Section 5 that this exceptional set has Hausdorff-dimension $2d-1$ in the $2d$-dimensional phase space and consequently its Lebesgue measure vanishes.

DOI: 10.1002/nme

Under the preceding assumptions, the action integral over the time interval $[t_0, t_2]$ follows as

$$I_h = \int_{t_0}^{t_2} L_h(q,\dot{q})\,\mathrm{d}t = \int_{t_0}^{t_1} L_h(q,\dot{q})\,\mathrm{d}t + \int_{t_1}^{t_2} L_h(q,\dot{q})\,\mathrm{d}t, \tag{5}$$

where t_1 is the time at which the trajectory intersects B_1. In regions where $V_h(q)$ is linear the trajectory $q(t)$ is quadratic in time. Therefore, the action of the system can be computed exactly and reduces to

$$\begin{aligned} I_h = {} & (t_1-t_0)\left\{\frac{1}{2}\left(\frac{q_1-q_0}{t_1-t_0}\right)^{\mathrm{T}} M \left(\frac{q_1-q_0}{t_1-t_0}\right)\right\} + (t_2-t_1)\left\{\frac{1}{2}\left(\frac{q_2-q_1}{t_2-t_1}\right)^{\mathrm{T}} M \left(\frac{q_2-q_1}{t_2-t_1}\right)\right\} \\ & -(t_1-t_0)\left\{V_I + \frac{1}{2}(q_1+q_0-2q_I)\cdot\nabla V_I + \frac{(t_1-t_0)^2}{24}\nabla V_I^{\mathrm{T}} M^{-1}\nabla V_I\right\} \\ & -(t_2-t_1)\left\{V_{II} + \frac{1}{2}(q_1+q_2-2q_{II})\cdot\nabla V_{II} + \frac{(t_2-t_1)^2}{24}\nabla V_{II}^{\mathrm{T}} M^{-1}\nabla V_{II}\right\}, \end{aligned} \tag{6}$$

where $q_1 = q(t_1)$ is constrained to be on the boundary surface B_1. Stationarity of the action with respect to (t_1, q_1) additionally gives the energy conservation equation

$$\begin{aligned} & \left(\frac{q_1-q_0}{t_1-t_0}\right)^{\mathrm{T}} M \left(\frac{q_1-q_0}{t_1-t_0}\right) + (q_0-q_1)\cdot\nabla V_I + \frac{(t_1-t_0)^2}{4}\nabla V_I^{\mathrm{T}} M^{-1}\nabla V_I \\ & \quad = \left(\frac{q_2-q_1}{t_2-t_1}\right)^{\mathrm{T}} M \left(\frac{q_2-q_1}{t_2-t_1}\right) + (q_2-q_1)\cdot\nabla V_{II} + \frac{(t_2-t_1)^2}{4}\nabla V_{II}^{\mathrm{T}} M^{-1}\nabla V_{II} \end{aligned} \tag{7}$$

and the linear momentum balance equation

$$M\frac{q_1-q_0}{t_1-t_0} - \frac{1}{2}(t_1-t_0)\nabla V_I - M\frac{q_2-q_1}{t_2-t_1} - \frac{1}{2}(t_2-t_1)\nabla V_{II} + \lambda n(q_1) = 0, \tag{8}$$

where λ is a Lagrange multiplier.

In order to make a more direct connection with time-integration schemes, we reformulate the problem slightly by assuming that t_0, q_0—the latter on a boundary surface B_0 except, possibly, at the initial time—and the initial velocity

$$\dot{q}_0^+ = \dot{q}(t_0^+) = \frac{q_1-q_0}{t_1-t_0} + \frac{1}{2}(t_1-t_0)M^{-1}\nabla V_I \tag{9}$$

are known. Let t_1 and q_1 be the time and point at which the trajectory intersects the next boundary surface B_1. We then seek to determine

$$\dot{q}_1^+ = \dot{q}(t_1^+) = \frac{q_2-q_1}{t_2-t_1} + \frac{1}{2}(t_2-t_1)M^{-1}\nabla V_{II}. \tag{10}$$

A reformulation of Equations (7) and (8) in terms of $\dot{q}_1^+$ gives

$$(\dot{q}_1^+)^{\mathrm{T}} M \dot{q}_1^+ = (\dot{q}_0^+)^{\mathrm{T}} M \dot{q}_0^+ - 2(q_1-q_0)\nabla V_I, \tag{11}$$

$$\dot{q}_1^+ = \dot{q}_0^+ - (t_1-t_0)\nabla V_I + \lambda M^{-1} n(q_1). \tag{12}$$

DOI: 10.1002/nme

Then, system (11–12) has the solution

$$\dot{q}_1 = \dot{q}(t_1^+) = \dot{q}(t_1^-) = \dot{q}_0^+ - (t_1 - t_0) M^{-1} \nabla V_I. \tag{13}$$

2.2. Stationary points of the action integral as weak solutions of the equation of motion

According to Hamilton's principle, the physical trajectories of a smooth Lagrangian system are the stationary points of the action integral $I = \int_0^{\mathrm{T}} L_h(q_h(t), \dot{q}_h(t))\,\mathrm{d}t$, $T > 0$. By analogy, the trajectories of an approximating Lagrangian L_h of the form (2) should emerge as critical points of the corresponding action functional I_h. We note that in the case of a continuous piecewise-linear potential energy the Lagrangian L_h is not differentiable everywhere and hence the notion of critical points does not have a well-defined meaning in the classical sense. However, the calculations in the previous subsection can be justified by interpreting the stationary points of the action integral I_h as weak solutions of the equation of motion. As shown in Section 5, for almost all initial conditions a discrete trajectory will not spend a positive amount of time in $\partial\mathscr{T}_h$, the union of element boundaries in $\mathscr{T}_h$. In order to derive the equation of motion, we will therefore restrict to such trajectories.

Theorem 2.1
Suppose $q_h \in W^{1,2}((0,T);\mathbb{R}^d)$ satisfies $|\{t : q_h(t) \in \partial\mathscr{T}_h\}| = 0$. Then, the action functional I_h is differentiable at q_h and q_h is a critical point of the action functional if and only if

$$M\ddot{q}_h(t) = -\nabla V_h(q_h(t)) \tag{14}$$

in the sense of distributions.

Note that the right hand of (14) is an element of $L^\infty((0,T);\mathbb{R}^d)$, hence q_h is a distributional solution of (14) if and only if $q_h \in W^{2,\infty}((0,T);\mathbb{R}^d)$ and $M\ddot{q}_h(t) = -\nabla V_h(q_h(t))$ holds almost everywhere.

Proof
Let $q_h, \varphi \in W^{1,2}((0,T);\mathbb{R}^d)$. Clearly, the first term in the first variation of I_h is

$$\lim_{\varepsilon\to 0} \frac{1}{2\varepsilon}\left(\int_0^{\mathrm{T}} (\dot{q}_h(t) + \varepsilon\dot{\varphi}(t))^{\mathrm{T}} M(\dot{q}_h(t) + \varepsilon\dot{\varphi}(t)) - \dot{q}_h^{\mathrm{T}}(t) M\dot{q}_h(t)\,\mathrm{d}t\right) = \int_0^{\mathrm{T}} \dot{q}_h^{\mathrm{T}}(t) M\dot{\varphi}(t)\,\mathrm{d}t. \tag{15}$$

On the other hand, if $|\{t : q_h(t) \in \partial\mathscr{T}_h\}| = 0$, then

$$\frac{1}{\varepsilon}(V_h(q_h(t) + \varepsilon\varphi(t)) - V_h(q_h(t))) \to \nabla V_h(q_h(t)) \cdot \varphi(t) \tag{16}$$

almost everywhere as $\varepsilon \to 0$. As V_h is locally Lipschitz, we furthermore have

$$\left|\frac{1}{\varepsilon} V_h(q_h(t) + \varepsilon\varphi(t)) - V_h(q_h(t))\right| \leqslant C\|\varphi\|_{L^\infty} \leqslant C\|\varphi\|_{W^{1,2}} \tag{17}$$

bounded independently of t. By dominated convergence we may therefore conclude that the second term in the first variation of I_h is

$$\lim_{\varepsilon\to 0} \frac{1}{\varepsilon} \int_0^{\mathrm{T}} (V_h(q_h(t) + \varepsilon\varphi(t)) - V_h(q_h(t)))\,\mathrm{d}t = \int_0^{\mathrm{T}} \nabla V_h(q_h(t)) \cdot \varphi(t)\,\mathrm{d}t. \tag{18}$$

DOI: 10.1002/nme

Summarizing, we have shown that the action functional is differentiable at q_h and that its derivative in direction φ is given by

$$\delta I_h(q,\varphi)=\int_0^{\mathrm{T}} \dot{q}_h^{\mathrm{T}}(t)M\dot{\varphi}(t)-\nabla V_h(q_h(t))\cdot\varphi(t)\,\mathrm{d}t. \tag{19}$$

This expression vanishes if and only if q_h is a weak solution to (14). □

2.3. Summary of the force-stepping scheme

We close this section by summarizing the relations obtained in the foregoing and by defining the *force-stepping* approximation scheme resulting from a continuous piecewise-linear approximation of the potential energy.

Definition 2.1 (*Force-stepping*)
Suppose $(t_k, q_k, \dot{q}_k)$ and a continuous piecewise-linear approximation of the potential energy V_h are given. Let t_{k+1} and q_{k+1} be the time and point of boundary crossing of the parabolic trajectory $q_k+(t-t_k)\dot{q}_k-\frac{1}{2}(t-t_k)^2M^{-1}\nabla V_k$. Then, the updated velocity is $\dot{q}_{k+1}=\dot{q}_k-(t_{k+1}-t_k)M^{-1}\nabla V_k$.

These relations define a discrete propagator

$$\Phi_h:(t_k,q_k,\dot{q}_k)\mapsto(t_{k+1},q_{k+1},\dot{q}_{k+1}) \tag{20}$$

that can be iterated to generate a discrete trajectory.

Algorithm 1 Force-stepping integrator

Require: $V(q)$, q_0, $\dot{q}_0$, t_0, t_f, $\Delta_0\in\mathscr{T}_h$, V_0 and ∇V_0
1: $k\leftarrow 0$
2: **while** $t_k<t_f$ **do**
3: $\{t_{k+1}, B_s\}\leftarrow$ TIME-STEP$(q_k,\dot{q}_k,\nabla V_k,t_k;\Delta_k)$
4: $q_{k+1}\leftarrow q_k+(t_{k+1}-t_k)\dot{q}_k-\frac{1}{2}(t_{k+1}-t_k)^2M^{-1}\nabla V_k$
5: $\dot{q}_{k+1}\leftarrow\dot{q}_k-(t_{k+1}-t_k)M^{-1}\nabla V_k$
6: $V_{k+1}\leftarrow V_k+(q_{k+1}-q_k)\cdot\nabla V_k$
7: $\{\nabla V_{k+1},\Delta_{k+1}\}\leftarrow$ UPDATE$(\nabla V_k,\Delta_k;B_s)$
8: $k\leftarrow k+1$
9: **end while**

The implementation of the force-stepping integrator is summarized in Algorithm 1. The algorithm consists of two methods. The first method TIME-STEP determines the time of exit of the parabolic trajectory from the simplex $\Delta_k\in\mathscr{T}_h$

$$q_k+(t_{k+1}-t_k)\dot{q}_k-\tfrac{1}{2}(t_{k+1}-t_k)^2M^{-1}\nabla V_k\in B_{\mathrm{s}}, \tag{21}$$

where $B_{\mathrm{s}}\in\partial\Delta_k$ is the boundary surface intersected. The second method UPDATE is responsible for updating all simplex-related information, e.g. ∇V_{k+1} of the adjacent simplex Δ_{k+1}. Both tasks can be effectively accomplished upon a unique, systematic, and efficient representation of the continuous piecewise-linear approximate potential energy, as presented in Section 3.

It bears emphasis that force-stepping requires the solution of no system of equations and, therefore, its complexity is comparable with that of explicit methods. However, the need to compute

DOI: 10.1002/nme

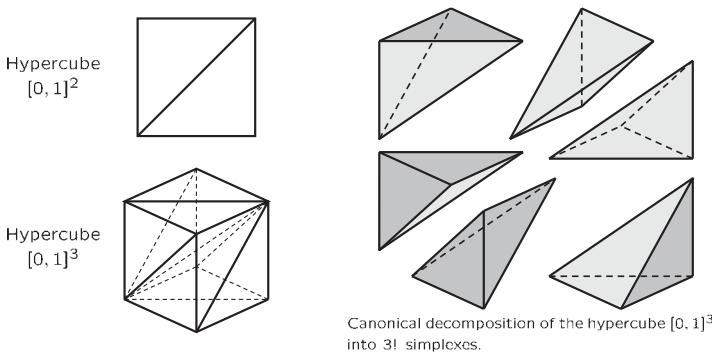

Figure 3. Simplicial partition of hypercubes $[0,1]^2$ and $[0,1]^3$.

the root of a non-linear function and to update all simplex-related information adds to the overhead of one application of the algorithm. It is still possible, however, that such overhead may be offset by the higher accuracy in particular applications. These and other trade-offs are investigated subsequently by way of numerical testing.

3. CONTINUOUS PIECEWISE LINEAR REPRESENTATION OF THE APPROXIMATE POTENTIAL V_h

One of the most successful applications of continuous piecewise-linear functions has been in non-linear circuit theory, in particular, in the field of non-linear resistive networks. In 1965, Katzenelson [6] presented an effective approach for the search of the operating point of a piecewise-linear resistive network. Since then, the same idea has been extended, improved and generalized [7–9]. Among these extensions and generalizations are the resolution of general non-linear equations of the form $f(x)=0$, where $f:\mathbb{R}^d\to\mathbb{R}^m$ is a continuous mapping [10], and the introduction of a canonical piecewise-linear function [11, 12] which allows for the compact and closed representation of any function using the minimal number of parameters by taking advantage of a simplicial partition of the domain [13].

Our aim in this section is to describe a unique, systematic, and efficient representation of the continuous piecewise-linear approximation of a function $f:\mathbb{R}^d\to\mathbb{R}$, in general, and the potential energy $V:\mathbb{R}^d\to\mathbb{R}$, in particular. With this goal in mind, we first consider a region $\mathscr{S}\subset\mathbb{R}^d$ and its regular tessellation in hyperrectangles or orthotopes with characteristic length $h_j\in\mathbb{R}^+$ in the jth direction, with $j=1,2,\ldots,d$. We then subdivide each hyperrectangle into proper simplices by introducing a unique, regular triangulation $\mathscr{T}_h$ in accordance with Chien and Kuh [7], see Figure 3. For later reference, we define the homeomorphism $\Lambda:\mathscr{S}\to\mathscr{S}_C$, represented by a diagonal matrix T, i.e. $z=Tq$, which maps hyperrectangles in $\mathscr{S}$ into hypercubes $[0,1]^d$ in a new region $\mathscr{S}_C\subset\mathbb{R}^d$. For alter reference, we name $\mathscr{V}$ and $\mathscr{V}_C$ the sets of vertices contained in regions $\mathscr{S}$ and $\mathscr{S}_C$, respectively.

Before we discuss further details of the continuous piecewise-linear representation of the approximate potential energy, we may first recall some properties of a simplex and its boundaries.

DOI: 10.1002/nme

Definition 3.1
Let $q^0, q^1, \ldots, q^d$ be $(d+1)$ points in general position in the d-dimensional space. A simplex $\Delta(q^0, q^1, \ldots, q^d)$ is defined as the convex hull of $q^0, q^1, \ldots, q^d$—the vertices of the simplex—

$$\Delta(q^0, q^1, \ldots, q^d) = \left\{ q : q = \sum_{i=0}^{d} \mu_i q^i, 1 \geqslant \mu_i \geqslant 0, i = 0, 1, 2, \ldots, d \text{ and } \sum_{i=0}^{d} \mu_i = 1 \right\}.$$

In addition, corresponding to the $(d+1)$ vertices, there are $(d+1)$ boundaries. The boundary B_s which corresponds to the vertex q^s is defined as

$$B_s = \{ q : q \in \Delta(q^0, q^1, \ldots, q^d) \text{ with } \mu_s = 0 \}.$$

As B_s contains all the vertices except q^s, there is a one-to-one correspondence between the vertices and the boundaries.

We now present the key steps for achieving a unique and systematic representation of force-stepping trajectories. To this end, we first subdivide each hypercube which belongs to $\mathscr{S}_C$ into non-overlapping simplices by properly arranging vertices of $\mathscr{V}_C$ in a fixed order [7]. This ordering relation allows for a unique representation of every point $z \in \mathscr{S}_C$ and $q \in \mathscr{S}$ (see Lemma 3.1). Therefore, there is a unique representation of the affine function $V_h(q) : \mathbb{R}^d \to \mathbb{R}$ with $V_h(q^i) = V(q^i)$ for all vertices $q^i \in \mathscr{V}$ (see Lemma 3.2) upon which force-stepping trajectories are systematically built.

Lemma 3.1
Every $z \in \mathscr{S}_C$ has a unique representation $z = \sum_{i=0}^{m} \mu_i z^i$, where $\mu_i > 0$, $z^i \in \mathscr{V}_C$, for $i = 0, 1, \ldots, m (\leqslant d)$, $\sum_{i=0}^{m} \mu_i = 1$, and the following ordering relation is attained $z^0 \leqslant z^1 \leqslant \cdots \leqslant z^m \leqq z^0 + 1$. Likewise, every $q \in \mathscr{S}$ has a unique representation $q = \sum_{i=0}^{m} \mu_i q^i$ where $q^i = T^{-1} z^i \in \mathscr{V}$, and the following ordering relation is attained $Tq^0 \leqslant Tq^1 \leqslant \cdots \leqslant Tq^m \leqq Tq^0 + 1$.

Proof
The proof in $\mathscr{S}_C$ is given by Kuhn [14]. The proof in $\mathscr{S}$ follows from the fact that the homeomorphism $\Lambda(\cdot)$ is defined by a positive-definite diagonal matrix T and therefore preserves the ordering of vertices. □

Corollary 3.1
If $m = d$, z is an interior point of the simplex $\Delta(z^0, z^1, \ldots, z^d)$. Otherwise, z lies on the boundary of a simplex. In addition, every d-dimensional simplex defined by $(d+1)$ vertices contains z^0 and $z^0 + 1$ which define the hypercube $C(z^0)$ containing the simplex.

Lemma 3.2
A non-linear function $V(q) : \mathbb{R}^d \to \mathbb{R}$ is approximated by an affine function $V_h(q) : \mathbb{R}^d \to \mathbb{R}$ as follows:

$$V_h(q) = \nabla V_\Delta \cdot q + V_0$$

DOI: 10.1002/nme

for $q \in \Delta(q^0, q^1, \ldots, q^d)$, $\nabla V_\Delta = \bar{J}_{h,[1\ldots d]} T \in \mathbb{R}^d$—the first d elements of the vector—and $V_0 = \bar{J}_{h,[d+1]} \in \mathbb{R}$. The Jacobian matrix of the piecewise-linear transformation is unique for a given simplex Δ and has the form

$$\bar{J}_h(q^0, q^1, \ldots, q^d) = (V(q^0) \ldots V(q^d)) \begin{pmatrix} Tq^0 & \ldots & Tq^d \\ 1 & \ldots & 1 \end{pmatrix}^{-1} =: V_\Delta Z_\Delta^{-1}$$

with $V_\Delta \in \mathbb{R}^{d+1}$ and $Z_\Delta^{-1} \in \mathbb{N}^{(d+1)\times(d+1)}$.

Proof
It follows from Lemma 3.1 that there is a unique representation of points $q \in \Delta(q^0, q^1, \ldots, q^d)$ and $z = Tq$ given by

$$\begin{pmatrix} z \\ 1 \end{pmatrix} = \begin{pmatrix} Tq \\ 1 \end{pmatrix} = \begin{pmatrix} Tq^0 & \ldots & Tq^d \\ 1 & \ldots & 1 \end{pmatrix} \mu = Z_\Delta \mu.$$

We now define the affine function $V_h(q)$, with $V_h(q^i) = V(q^i)$ for $i = 0, 1, \ldots, d$, as

$$V_h(q) = (V(q^0) \ldots V(q^d)) \cdot \mu = V_\Delta Z_\Delta^{-1} \cdot \begin{pmatrix} z \\ 1 \end{pmatrix} = \bar{J}_h \cdot \begin{pmatrix} Tq \\ 1 \end{pmatrix}.$$

Then, the claim follows from writing the affine function as $V_h(q) = \nabla V_\Delta \cdot q + V_0$. We note that both matrices Z_Δ and Z_Δ^{-1} belong to $\mathbb{N}^{(d+1)\times(d+1)}$ due to the fact that hypercubes in $\mathscr{S}_C$ have unit volume, i.e. $\det(Z_\Delta) = 1$. □

We then show that force-stepping trajectories $\{t_k, q_k, \dot{q}_k\}$, as described in Definition 2.1, can be systematically tracked in phase space. In particular, we show that successive times of boundary crossings $t_0 < t_1 < t_2 < \ldots$ and the corresponding sequence of positions $q_0, q_1, q_2, \ldots$ can be obtained from the simplicial partition presented above. The procedure applied for solving this problem, namely *the time-step problem* (see Proposition 3.1), is indeed the method TIME-STEP required by the implementation of the force-stepping integrator presented in Algorithm 1,

$$\{t_{k+1}, B_s\} \leftarrow \text{TIME-STEP}(q_k, \dot{q}_k, \nabla V_k, t_k; Z_{\Delta_k}^{-1}).$$

Proposition 3.1 (*The time-step problem*)
A general trajectory of the form $q(t) = q_k + (t - t_k)\dot{q}_k - \frac{1}{2}(t - t_k)^2 M^{-1} \nabla V_k$, with $q(t_k^+) \in \Delta(q^0, q^1, \ldots, q^d)$ and $t > t_k$, intersects the boundary B_s of the simplex $\Delta(q^0, q^1, \ldots, q^d)$ at $q(t_{k+1}) = q_{k+1}$ with

$$t_{k+1} = \min_{r \in [0,d]} \inf\{t > t_k : \mu_{1,r} + (t - t_k)\mu_{2,r} + (t - t_k)^2 \mu_{3,r} = 0\},$$

$$s = \arg \min_{r \in [0,d]} \{\mu_{1,r} + (t_{k+1} - t_k)\mu_{2,r} + (t_{k+1} - t_k)^2 \mu_{3,r} = 0\},$$

where

$$(\mu_1 \mid \mu_2 \mid \mu_3) = Z_\Delta^{-1} \left(\begin{array}{c|c|c} Tq_k & T\dot{q}_k & -M^{-1} T \nabla V_k / 2 \\ 1 & 0 & 0 \end{array} \right).$$

DOI: 10.1002/nme

Proof
It follows from Definition 3.1 and Lemma 3.1 that a trajectory of the form $q(t)=\sum_{r=0}^{d}\mu_r(t)q^r$, with $q(t_k^+)\in\Delta(q^0,q^1,\ldots,q^d)$ and $t>t_k$, intersects the boundary B_{r^*} of the simplex $\Delta(q^0,q^1,\ldots,q^d)$ at $q(t^*)$ if and only if the r^*th component of $\mu(t^*)$ is equal to zero with all other components positive. Then, the following equality holds

$$\mu(t)=Z_\Delta^{-1}\begin{pmatrix}Tq(t)\\1\end{pmatrix}=\underbrace{Z_\Delta^{-1}\begin{pmatrix}Tq_k\\1\end{pmatrix}}_{\mu_1\in\mathbb{R}^{d+1}}+(t-t_k)\underbrace{Z_\Delta^{-1}\begin{pmatrix}T\dot{q}_k\\0\end{pmatrix}}_{\mu_2\in\mathbb{R}^{d+1}}+(t-t_k)^2\underbrace{Z_\Delta^{-1}\begin{pmatrix}-M^{-1}T\nabla V_k/2\\0\end{pmatrix}}_{\mu_3\in\mathbb{R}^{d+1}}$$

and the claim follows from the fact that t_{k+1} is the earliest $t^*>t_k$ for which $\mu_{r^*=s}(t^*)=0$ among all possible pairs (t^*,r^*). □

It is worth noting that the representation of the approximate potential energy V_h can be restricted solely to the current simplex Δ_k and the relevant simplex-related matrices are $\langle V_{\Delta_k},Z_{\Delta_k},Z_{\Delta_k}^{-1}\rangle$, with

$$V_{\Delta_k}=(V(q^0)\ \ldots\ V(q^s)\ \ldots\ V(q^d)),$$
$$Z_{\Delta_k}=\begin{pmatrix}z^0&\ldots&z^s&\ldots&z^d\\1&\ldots&1&\ldots&1\end{pmatrix}.$$

We then claim that *the replacement rule* (see Chien and Kuh [7] and Lemma 3.3) provides for a very efficient scheme to construct the adjacent simplex Δ_{k+1} knowing only the boundary B_s of the current simplex Δ_k intersected by the trajectory. Moreover, we describe an efficient procedure for updating all simplex-related matrices required to compute the force-stepping trajectory in Δ_{k+1}. In particular, given all Δ_k-related matrices and the intersected boundary B_s, matrices are updated as follows:

$$V_{\Delta_{k+1}}=(V(q^0)\ldots V(q'^s)\ldots V(q^d)),$$
$$Z_{\Delta_{k+1}}=\begin{pmatrix}z^0&\ldots&z'^s&\ldots&z^d\\1&\ldots&1&\ldots&1\end{pmatrix},$$
$$Z_{\Delta_{k+1}}^{-1}=Z_{\Delta_k}^{-1}-\frac{(Z_{\Delta_k}^{-1}u^s)\otimes(v^sZ_{\Delta_k}^{-1})}{1+v^sZ_{\Delta_k}^{-1}u^s},$$

where $z'^s=z^{s+1}+z^{s-1}-z^s$, $q'^s=T^{-1}z'^s$, $u^s=z'^s-z^s$, and $v_i^s=\delta_{i,s}$. Matrices $Z_{\Delta_{k+1}}$ and $V_{\Delta_{k+1}}$ are obtained by replacing z^s with z'^s and $V(q^s)$ with $V(q'^s)$, respectively. The matrix $Z_{\Delta_{k+1}}^{-1}$ is 1-rank updated by means of the Sherman–Morrison formula [15]—with algorithm complexity $O(d^2)$—instead of computing the inverse of $Z_{\Delta_{k+1}}$—with algorithm complexity $O(d^3)$. The overall gain in efficiency is remarkable.

Lemma 3.3 (*The replacement rule*)
Let B_s be the boundary shared by two adjacent simplices. Given the simplex $\Delta(q^0,q^1,\ldots,q^{s-1},q^s,q^{s+1},\ldots,q^d)$, with $Tq^0\leqslant Tq^1\leqslant\cdots\leqslant Tq^d$, its neighbor is simply defined by replacing q^s with q'^s.

DOI: 10.1002/nme

The new vertex is defined as

$$q'^s = q^{s+1} + q^{s-1} - q^s,$$

where $q^{d+1} \equiv q^0$ and $q^{-1} \equiv q^d$.

Corollary 3.2
The replacement rule preserves the order in the set of vertices $\mathscr{V}$.

Proof
For $s = 1, \ldots, d-1$, the following relation holds $Tq^{s-1} \leqslant Tq'^s \leqslant Tq^{s+1}$. For $s = 0$ ($s = d$) a simple backward (forward) shift of indices has to be introduced in the updated set of vertices. After the shift is performed, the new set of vertices verifies the ordering relation. □

We conclude this section with the second method required by the implementation of the force-stepping integrator presented in Algorithm 1

$$\{\nabla V_{k+1}, \langle V_{\Delta_{k+1}}, Z_{\Delta_{k+1}}, Z^{-1}_{\Delta_{k+1}} \rangle\} \leftarrow \textsc{Update}(\nabla V_k, \langle V_{\Delta_k}, Z_{\Delta_k}, Z^{-1}_{\Delta_k} \rangle; B_s).$$

The method is defined in Algorithm 2 and is responsible for applying *the replacement rule* as well as updating ∇V_k and all simplex-related matrices $\langle V_{\Delta_k}, Z_{\Delta_k}, Z^{-1}_{\Delta_k} \rangle$. These tasks are achieved with computational complexity $O(d^2)$, as opposed to $O(d^3)$ for implicit methods. We remark that, for all practical purposes, there is no need to shift indices after vertices q^0 or q^d are updated by the algorithm, as suggested by Corollary 3.2.

Algorithm 2 $\textsc{Update}(\nabla V_k, \langle V_{\Delta_k}, Z_{\Delta_k}, Z^{-1}_{\Delta_k} \rangle; B_s)$

Require: $z'^s = z^{s+1} + z^{s-1} - z^s$, $u^s = z'^s - z^s$, $v^s_i = \delta_{i,s}$ and $q'^s = T^{-1} z'^s$

1: $Z^{-1}_{\Delta_{k+1}} \leftarrow Z^{-1}_{\Delta_k} - \frac{(Z^{-1}_{\Delta_k} u^s) \otimes (v^s Z^{-1}_{\Delta_k})}{1 + v^s Z^{-1}_{\Delta_k} u^s}$

2: $Z_{\Delta_{k+1}} \leftarrow \begin{pmatrix} z^0 & \cdots & z'^s & \cdots & z^d \\ 1 & \cdots & 1 & \cdots & 1 \end{pmatrix}$

3: $V_{\Delta_{k+1}} \leftarrow \begin{pmatrix} V(q^0) & \cdots & V(q'^s) & \cdots & V(q^d) \end{pmatrix}$

4: $\bar{J}_h \leftarrow V_{\Delta_{k+1}} Z^{-1}_{\Delta_{k+1}}$

5: $\nabla V_{k+1} \leftarrow \bar{J}_{h,[1\ldots d]} T$

6: **return** $\nabla V_{k+1}, \langle V_{\Delta_{k+1}}, Z_{\Delta_{k+1}}, Z^{-1}_{\Delta_{k+1}} \rangle$

4. CONSERVATION PROPERTIES

Some symmetries of Lagrangian systems, such as time-reversal, parity and invariance under time shifts in the particular case of autonomous or time-independent systems, are preserved upon piecewise-linear approximation of the potential energy, which results in the exact conservation of the corresponding momentum maps. In particular, force-stepping trajectories conserve energy exactly. In contrast, and unlike energy-stepping, which results in exact conservation of all momenta,

DOI: 10.1002/nme

piecewise-linear approximation may break some symmetries of the potential energy, such as translation and rotation invariance, resulting in a lack of exact conservation of the corresponding momenta. However, in this section we show that the force-stepping scheme is nearly conserving for all symmetries of the system, whether explicitly known or otherwise. The numerical experiments presented in Section 6 further show that the corresponding momentum maps tend to remain nearly uniformly constant for all times. We also show that some broken symmetries can be restored exactly by recourse to Lagrangian reduction.

4.1. Conservation of momentum maps

We recall (cf., e.g. [16]) that a general Lagrangian is a function $L : TQ \to \mathbb{R}$, where Q is a smooth manifold, known as configuration manifold, and TQ is the corresponding tangent bundle, consisting of pairs of configurations and velocities. For simplicity, we restrict attention to time-independent or autonomous Lagrangians. Let X denote some suitable topological space of trajectories $q : [0, T] \to Q$ joining fixed initial and final configurations $q(0)$ and $q(T)$, respectively. Then, the action integral $I : X \to \mathbb{R}$ over the time interval $[0, T]$ is

$$I(q) = \int_0^T L(q(t), \dot{q}(t))\,\mathrm{d}t, \tag{22}$$

where we assume sufficient regularity of L and $q(t)$ for all mathematical operations to be well defined. According to Hamilton's principle, the physical trajectories of the system are the critical points of I, i.e. $q \in X$ is a trajectory if

$$\delta I(q, \varphi) = 0 \tag{23}$$

for all variations $\varphi \in C_c^\infty(0, T)$. Throughout the present work the configurational space of interest is $Q = E(n)^N$, where $E(n)$ is the Euclidean space of dimension n (i.e. $d = nN$), and the Lagrangian is assumed to be of the form (1), with V smooth and bounded below, or (2) with V_h continuous piecewise-linear. An appropriate space of trajectories is $X = W^{2,\infty}_{\mathrm{loc}}([0, \infty))$, as demonstrated in Section 5. We note that in the case of a continuous piecewise-linear potential energy the Euler–Lagrange equations are not defined in the classical sense. However, the trajectories can still be understood as critical points of the action functional I_h as shown in Theorem 2.1. In particular, on element boundaries the acceleration is not uniquely defined. However, we show in Section 5 that, for almost all initial conditions, simplex boundaries are crossed only at isolated points in time, and for those initial conditions the discrete trajectories are well defined and convergent.

Let G be a Lie group with Lie algebra $\mathfrak{g} = T_e G$. A left action of G on Q is a mapping $\Phi : G \times Q \to Q$ such that: (i) $\Phi(e, \cdot) = \mathrm{id}$; (ii) $\Phi(g, \Phi(h, \cdot)) = \Phi(gh, \cdot)\ \forall g, h \in G$. Let $\xi \in \mathfrak{g}$. Then, the infinitesimal generator of Φ corresponding to ξ is the vector field $\xi_Q \in TQ$ given by

$$\xi_Q(q) = \frac{\mathrm{d}}{\mathrm{d}t}[\Phi(\exp(t\xi), q)]_{t=0}. \tag{24}$$

The momentum map $J : TQ \to \mathfrak{g}^*$ defined by the action Φ then follows from the identity

$$\langle J(q, \dot{q}), \xi \rangle = \langle \partial_{\dot{q}} L(q, \dot{q}), \xi_Q(q) \rangle \quad \forall \xi \in \mathfrak{g}. \tag{25}$$

We say that the Lagrangian L is invariant under the action Φ if

$$L(\Phi_g(q), T\Phi_g(q)\dot{q}) = L(q, \dot{q}) \quad \forall g \in G, (q, \dot{q}) \in TQ, \tag{26}$$

DOI: 10.1002/nme

where we write $\Phi_g(\cdot)=\Phi(g,\cdot)$. Under these conditions, we additionally say that G is a symmetry group of the system and that Φ expresses a symmetry of the system.

The classical theorem of Noether states that if L is invariant under the action Φ, then the corresponding momentum map J is a constant of the motion, i.e. it remains constant along trajectories. Classical examples include:

(i) Conservation of linear momentum. In this case, $Q=E(n)^N$, $G=E(n)$, and $\Phi(u,q)=\{q_1+u,\ldots,q_N+u\}$ represent a rigid translation of the system by $u\in E(n)$. The corresponding momentum map is the total linear momentum of the system, $J=p_1+\cdots+p_N$. If the Lagrangian is invariant under translations, then the total linear momentum is a constant of the motion.

(ii) Conservation of angular momentum. In this case, $Q=E(n)^N$, $G=SO(n)$, and $\Phi(R,q)=\{Rq_1,\ldots,Rq_N\}$ represent a rigid rotation of the system by $u\in SO(n)$. The corresponding momentum map is the total angular momentum of the system, $J=q_1\times p_1+\cdots+q_N\times p_N$. If the Lagrangian is invariant under rotations, then the total angular momentum is a constant of the motion.

Conservation of energy can be fit into this framework by recourse to a space–time formulation in which time is regarded as a generalized coordinate, e.g. q_0. The corresponding space–time Lagrangian is $\mathbb{L}(\mathbb{q},\mathbb{q}')=\mathbb{L}((q_0,q),(q_0',q'))=L(q,q'/q_0',q_0)$, where $L(q,\dot{q},t)$ is a general time-dependent Lagrangian. The space–time configuration manifold is $\mathbb{R}\times Q$. Let $G=\mathbb{R}$, $\Phi(s,q)=(q_0+s,q)$ is a time-shift and suppose that $\mathbb{L}$ is invariant under Φ, i.e. L is time-independent. Then $J=L-\partial_{\dot{q}}L\cdot\dot{q}=-E$, i.e. the total energy of the system, is a constant of the motion. However, exact energy conservation follows more directly as a consequence of (11), i.e. energy conservation is built explicitly into the force-stepping scheme.

Evidently, a naïve continuous piecewise-linear approximation of the potential energy breaks the symmetries of the system in general, including translation and rotation invariance. Thus, if G is a symmetry group of V and Φ is an action that leaves V invariant, the corresponding momentum map J may not be constant along force-stepping trajectories in general. This lack of exact conservation can be remedied by recourse to Lagrangian reduction, as shown subsequently. However, even the naïve force-stepping scheme, with no symmetrization of the approximated potential, has near-conservation properties, as shown next.

Theorem 4.1

Suppose that G is a symmetry group of the potential V, i.e. $V\circ\Phi_g=V$ for all $g\in G$, and let $J(q,\dot{q})$ be the corresponding momentum map. Let $q_0,\dot{q}_0\in\mathbb{R}^{nN}$ and $h_m\to 0$. Suppose, in addition, that $q_{h_m}\in W^{2,\infty}(0,T)$ are force-stepping trajectories corresponding to the approximate potentials V_{h_m} and q is a trajectory corresponding to the original potential V, with $q(0)=q_{h_m}(0)=q_0$ and $\dot{q}(0)=\dot{q}_{h_m}(0)=\dot{q}_0$ for all m. Then we have $J(q_{h_m},\dot{q}_{h_m})\to J(q,\dot{q})\equiv J(q_0,\dot{q}_0)$ in $W^{1,\infty}_{\mathrm{loc}}([0,\infty))$ for almost all initial conditions $(q_0,\dot{q}_0)$.

Proof

From Theorem 5.2 we deduce that, except for a $(2nN-1)$-dimensional set of initial conditions $(q_0,\dot{q}_0)$, q_{h_m} converges to the continuum solution q strongly in $W^{2,\infty}_{\mathrm{loc}}([0,\infty))$. As L and, thus, J are smooth this implies that $J(q_{h_m},\dot{q}_{h_m})\to J(q,\dot{q})$ in $W^{1,\infty}_{\mathrm{loc}}([0,\infty))$. As J is conserved along the continuum trajectory $(q,\dot{q})$, i.e. $J(q,\dot{q})\equiv J(q_0,\dot{q}_0)$, the claim follows. □

DOI: 10.1002/nme

It is interesting to note that an *approximate Noether theorem* can also be obtained for general potentials, and not just those resulting by approximation of a symmetric potential. We state it here for smooth potentials and compact *almost-symmetry groups*. In order to quantify the extent to which a Lagrangian L fails to be symmetric with respect to a Lie group G acting on Q via Φ, we introduce the functions

$$L_g(q,\dot{q}) = L(\Phi_g(q), T\Phi_g(q)\dot{q}) \tag{27}$$

parameterized by $g \in G$. In the symmetric case, $L_g = L_e = L$ exactly. The following theorem shows that, for an approximate conservation estimate, we require that $L_g \sim L$ up to first order in q and up to second order in $\dot{q}$. In particular, these assumptions are satisfied for the piecewise-linear Lagrangians (2), which approximate the original Lagrangian (1) to first order in q and to second order in $\dot{q}$.

Theorem 4.2 (*Approximate Noether's theorem*)
Suppose G is a compact Lie group and Φ is a smooth left action of G on Q with momentum map J. Let $U \subset TQ$ be relatively compact and assume that L is uniformly strictly convex on U with respect to $\dot{q}$. Suppose (near symmetry) that

$$\sup_{g\in G}\left(\|L - L_g\|_{L^\infty(U)} + \left\| \frac{\partial L}{\partial q} - \frac{\partial L_g}{\partial q} \right\|_{L^\infty(U)} + \left\| \frac{\partial L}{\partial \dot{q}} - \frac{\partial L_g}{\partial \dot{q}} \right\|_{L^\infty(U)} + \|\nabla^2_{\dot{q}} L - \nabla^2_{\dot{q}} L_g\|_{L^\infty(U)} \right) \leqslant \varepsilon. \tag{28}$$

Then, for all trajectories $(q,\dot{q})$ such that $(q(t),\dot{q}(t)) \in \overline{U}$ for $t \in [0,T]$, there exists a constant $C>0$ such that

$$\|J(q,\dot{q}) - J(q_0,\dot{q}_0)\|_{W^{1,\infty}([0,T])} \leqslant C\varepsilon. \tag{29}$$

Note that for Lagrangians of the form (1), for given T, q_0, and $\dot{q}_0$ one can find a relatively compact set U satsifying $(q(t),\dot{q}) \in U$ for all $t \in [0,T]$ which only depends on the minimum value of V. This is easily deduced from energy conservation.

Proof
Define the symmetrized Lagrangian L' by

$$L'(q,\dot{q}) := \fint_G L(\Phi_g(q), T\Phi_g(q)\dot{q})\,\mathrm{d}g, \tag{30}$$

where $\fint_G(\cdots)\,\mathrm{d}g = \frac{1}{|G|}\int_G(\cdots)\,\mathrm{d}g$ denotes the normalized integration with respect to the right invariant Haar measure of G. Then L' is invariant under Φ since

$$\begin{aligned} L'(\Phi_{\tilde{g}}(q), T\Phi_{\tilde{g}}(q)\dot{q}) &= \fint_G L(\Phi_g(\Phi_{\tilde{g}}(q)), T\Phi_g(\Phi_{\tilde{g}}(q)) T\Phi_{\tilde{g}}(q)\dot{q})\,\mathrm{d}g \\ &= \fint_G L(\Phi_{g\tilde{g}}(q), T\Phi_{g\tilde{g}}(q)\dot{q})\,\mathrm{d}g = \fint_G L(\Phi_g(q), T\Phi_g(q)\dot{q})\,\mathrm{d}g = L'(q,\dot{q}) \end{aligned}$$

DOI: 10.1002/nme

for all $\tilde{g} \in G$. By Noether's Theorem we thus conclude that the momentum map J' corresponding to L' is conserved along trajectories q' corresponding to the Lagrangian L', i.e. on paths satisfying

$$\frac{\partial L'}{\partial q}(q'(t)) - \frac{\mathrm{d}}{\mathrm{d}t}\frac{\partial L'}{\partial \dot{q}}(q'(t)) = 0. \tag{31}$$

Now we have, by assumption,

$$\|L - L'\|_{L^\infty(U)} = \left\| \fint_G (L - L_g)\,\mathrm{d}g \right\|_{L^\infty(U)} \leqslant \fint_G \|L - L_g\|_{L^\infty(U)}\,\mathrm{d}g \leqslant \varepsilon, \tag{32}$$

since $\fint_G 1\,\mathrm{d}g = 1$. In addition,

$$\left\| \frac{\partial L}{\partial q} - \frac{\partial L'}{\partial q} \right\|_{L^\infty(U)} = \left\| \fint_G \left(\frac{\partial L}{\partial q} - \frac{\partial L_g}{\partial q} \right) \mathrm{d}g \right\|_{L^\infty(U)} \leqslant \fint_G \left\| \frac{\partial L}{\partial q} - \frac{\partial L_g}{\partial q} \right\|_{L^\infty(U)} \mathrm{d}g \leqslant \varepsilon \tag{33}$$

and, similarly,

$$\left\| \frac{\partial L}{\partial \dot{q}} - \frac{\partial L'}{\partial \dot{q}} \right\|_{L^\infty(U)} \leqslant \varepsilon \quad \text{and} \quad \|\nabla^2_{\dot{q}} L - \nabla^2_{\dot{q}} L'\|_{L^\infty(U)} \leqslant \varepsilon. \tag{34}$$

Also by assumption, the Hessian $\nabla^2_{\dot{q}} L$ is uniformly non-singular. The previous estimate (34) shows that this is also true for $\nabla^2_{\dot{q}} L'$, as we may, without loss of generality, assume that ε is sufficiently small. As a consequence, we obtain that the solutions q and q' of

$$\frac{\partial L}{\partial q}(q(t)) - \frac{\mathrm{d}}{\mathrm{d}t}\frac{\partial L}{\partial \dot{q}}(q(t)) = 0 \quad \text{resp.} \quad \frac{\partial L'}{\partial q}(q'(t)) - \frac{\mathrm{d}}{\mathrm{d}t}\frac{\partial L'}{\partial \dot{q}}(q'(t)) = 0$$

subject to the same initial conditions $q(0) = q'(0) = q_0$, $\dot{q}(0) = \dot{q}'(0) = \dot{q}_0$ satisfy the estimate

$$\|q - q'\|_{W^{2,\infty}(0,T)} \leqslant C\varepsilon. \tag{35}$$

Another consequence of the above estimates (32), (33), and (34) is that, since by (25) the momentum maps J and J' depend smoothly on $\partial_{\dot{q}} L$ and $\partial_{\dot{q}} L'$, respectively,

$$\|J - J'\|_{W^{1,\infty}(U)} \leqslant \|L - L'\|_{W^{1,\infty}(U)} \leqslant C\varepsilon. \tag{36}$$

Finally, from (35) and (36) it follows that

$$\begin{aligned} &\|J(q,\dot{q}) - J(q_0,\dot{q}_0)\|_{W^{1,\infty}(0,T)} \\ &\leqslant \|J(q,\dot{q}) - J'(q',\dot{q}')\|_{W^{1,\infty}(0,T)} + \|J'(q_0,\dot{q}_0) - J(q_0,\dot{q}_0)\|_{W^{1,\infty}(0,T)} \leqslant C\varepsilon. \end{aligned}$$

□

In essence, the preceding theorem states that almost-symmetries, in the sense of (28), result in almost-conservation in the sense of (29). The theorem thus effectively removes the rigidity of the classical Noether's theorem, which applies to exact symmetries only.

DOI: 10.1002/nme

4.2. Lagrangian reduction

A general strategy for avoiding broken symmetries in the force-stepping scheme is supplied by the theory of Lagrangian reduction. The aim of this theory is to reduce the dimension of the configuration space of a Lagrangian by systematically exploiting constants of motion and symmetry groups (cf., e.g. [16, 17] and references therein). Thus, suppose G is a Lie group, $L : TQ \to \mathbb{R}$ is a Lagrangian invariant under a smooth left action Φ of G on Q, with momentum map J. Then, the theory defines a reduced Lagrangian $l : TQ/G \to \mathbb{R}$ in which the group coordinates are eliminated. Classical examples include:

(i) *Total linear momentum*. In this case, $Q = E(n)^N$, $G = E(n)$ and $J = p_1 + \cdots + p_N$. Then, given a total linear momentum $\mu \in \mathfrak{g}^*$, the isotropy group G_μ, i.e. the group of actions that leaves the level set $J^{-1}(\mu)$ invariant, reduces to $G_\mu = G$. Thus, the corresponding reduced phase space is given by $J^{-1}(\mu)/G_\mu = T(E(n)^{N-1})$ and has dimension $2n(N-1)$.

(ii) *Total angular momentum* ($n = 3, N \geqslant 3$). In this case, $Q = E(3)^N$, $G = SO(3)$ and $J = q_1 \times p_1 + \ldots + q_N \times p_N$. Then, given a total angular momentum $\mu \in \mathfrak{g}^*$, the dimension of the corresponding reduced phase space $J^{-1}(\mu)/G_\mu$ depends on the value of μ. For $\mu = 0$, any rotation leaves the level set $J^{-1}(0)$ invariant, that is $G_\mu = G$, and therefore the reduced phase space has dimension $6(N-1)$. For $\mu \neq 0$, only rotations along the direction of μ leave the level set $J^{-1}(\mu)$ invariant, that is $G_\mu = S^1$, and therefore the reduced phase space has dimension $6N-4$.

(iii) *Total linear and angular momenta* ($n = 3$, $N \geqslant 3$). Given a total linear momentum μ_1 and a total angular momentum μ_2, one concludes from the preceding analysis that the corresponding reduced phase space TQ/G has dimension $6N-12$, resp. $6N-10$, for $\mu_2 = 0$, resp. $\mu_2 \neq 0$.

The reduced Lagrangian resulting from the elimination of constrained degrees of freedom represents the intrinsic or internal dynamics of the system. Furthermore, the reduced Lagrangian implicitly inherits the conservations laws of the original system. In addition, it is possible to reconstruct the original dynamics from the reduced dynamics.

As an application of the theory, consider Lagrangians of the form (1) with diagonal mass matrix M and potential V, invariant under translations and rotations. Such systems are known as N-body problems and are the subject of a vast body of literature (cf., e.g. [18–22]). Reduction with respect to translational symmetry may be achieved by recourse to Jacobi coordinates $q' \in E(n)^{N-1}$ and center of mass coordinates $q_{cm} \in E(n)$, defined as

$$q'_j = q_{j+1} - \frac{\sum_{i=1}^{j} m_i q_i}{\sum_{i=1}^{j} m_i}, \quad 1 \leqslant j < N, \tag{37}$$

$$q_{cm} = \frac{\sum_{i=1}^{N} m_i q_i}{m_T}, \tag{38}$$

where m_i is the mass of the ith particle and

$$m_T = \sum_{i=1}^{N} m_i \tag{39}$$

DOI: 10.1002/nme

is the total mass of the system. Clearly, the map $\pi: q \to (q', q_{cm})$ is linear and bijective, and its inverse $\pi^{-1}(q', q_{cm}) \to q$ is given by

$$q_j = q_{cm} + q'_{j-1} \frac{\sum_{i=1}^{j-1} m_i}{\sum_{i=1}^{j} m_i} - \sum_{i=j+1}^{N} \frac{m_i q'_{i-1}}{\sum_{k=1}^{i} m_k}, \quad 1 \leqslant j \leqslant N, \tag{40}$$

with $q'_0 = 0$. The corresponding constant of the motion is the total linear momentum $\mu_1 = \sum_{i=1}^{N} m_i \dot{q}_i$ and the reduced Lagrangian

$$l(q', \dot{q}') = \tfrac{1}{2} \dot{q}'^{\mathrm{T}} M' \dot{q}' - V'(q') \tag{41}$$

retains the desirable form (1). It is readily shown that the reduced mass matrix M' is diagonal with non-zero elements

$$m'_j = m_{j+1} \frac{\sum_{i=1}^{j} m_i}{\sum_{i=1}^{j+1} m_i} \tag{42}$$

and that the reduced potential is

$$V'(q') = V(\pi^{-1}(q', 0)). \tag{43}$$

It should be carefully noted that the evolution of the center of mass $q_{cm}(t)$ is decoupled from the dynamics of the reduced system and, as part of the reconstruction of the original dynamics, it can be trivially obtained as

$$\dot{q}_{cm} = \frac{\mu_1}{m_T}. \tag{44}$$

The trajectories of the reduced Lagrangian system can now be approximated by replacing (41) by an approximate reduced Lagrangian $l_h(q', \dot{q}')$ that can be solved exactly, e.g. of the form

$$l_h(q', \dot{q}') = \tfrac{1}{2} \dot{q}'^{\mathrm{T}} M' \dot{q}' - V'_h(q'). \tag{45}$$

obtained by replacing V' by its piecewise-linear approximation V'_h. By this construction, the approximate Lagrangian l_h is translation invariant and the total linear momentum is exactly conserved along the corresponding trajectories.

The reduction with respect to the rotational symmetry, in applications which involve an arbitrary number of particles ($N \geqslant 3$) and non-vanishing angular momentum, is presently the subject of active research (cf., e.g. [19–22]). Unfortunately, it is not possible to construct internal or shape coordinates which result in a reduced Lagrangian of the form (1).

4.3. Conservation of discrete symmetries

Lagrangian systems may also have some symmetries that are associated with actions of *discrete* groups rather than with actions of *continuous* groups—Lie groups G presented in the previous subsections are continuous. This is the case of many non-relativistic systems which are invariant under parity. Parity is a discrete symmetry expressed by an operator P, whose action on configuration space $Q = E(3)^N$ is given by $Pq_j = -q_j$, and on $Q = E(2)^N$ is given by flipping the sign of only one component of q_j. In general, G-invariant reductions may or may not preserve the parity

DOI: 10.1002/nme

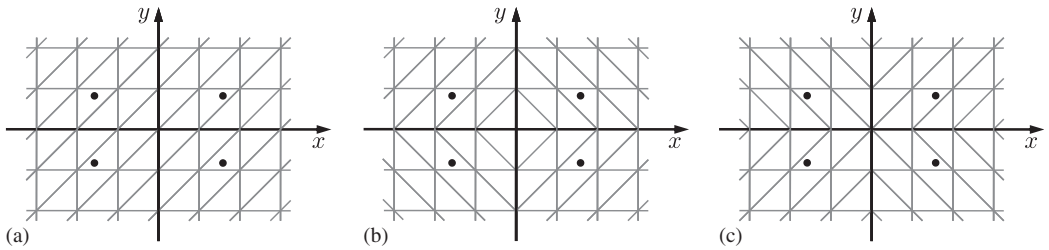

Figure 4. Three feasible regular triangulations of $\mathbb{R}^2$. Triangulation (a) breaks the parity invariance of $V(q)$; triangulations (b); and (c), do not.

symmetry P. However, reductions with respect to translations given by the map $\pi(q)$, (37)–(38), induce effective potentials $V'(q')$ invariant under parity, that is $V'(Pq')=V'(q')$.

In applications, we employ regular triangulations $\mathscr{T}_h$ which result in piecewise-affine approximate potentials V'_h invariant under parity. Figure 4 illustrates the simple case of $Q'=E(2)$. The extension to $Q'=E(n)^{N-1}$ is straightforward and falls squarely within the construction presented in Section 3. In addition, time-reversibility follows directly from the definition of the force-stepping scheme. The time-reversal symmetry of Lagrangian systems is a discrete symmetry that is widely considered to be essential to the design of efficient time-integration schemes (cf., e.g. [23] and references therein).

4.4. Conservation of the symplectic structure

In order to establish the symplecticity of the force-stepping scheme, we proceed to look at the Lagrangian system defined by (1) from a Hamiltonian perspective. To this end, we introduce the phase space $P=T^*Q$, consisting of pairs (q,p) of configurations $q\in Q=E(n)^N$ and momenta $p\in T^*_qQ$, and the Hamiltonian $H:P\to\mathbb{R}$ as

$$H(q,p)=\sup_{v\in T_qQ}\{p\cdot v-L(q,v)\}=\frac{1}{2}p^{\mathrm{T}}M^{-1}p+V(q). \tag{46}$$

For a G-invariant reduced Lagrangian defined by (41), we also introduce the reduced Hamiltonian $H_\mu:P_\mu\to\mathbb{R}$ as

$$H_\mu(q',p')=\sup_{v\in T_{q'}Q/G}\{p'\cdot v-l(q',v)\}=\frac{1}{2}p'^{\mathrm{T}}M'^{-1}p'+V'(q'). \tag{47}$$

Likewise, the Hamiltonian corresponding to the approximate reduced Lagrangian (45) is

$$H_{\mu,h}(q',p')=\sup_{v\in T_{q'}Q/G}\{p'\cdot v-l_h(q',v)\}=\frac{1}{2}p'^{\mathrm{T}}M'^{-1}p'+V'_h(q'). \tag{48}$$

We now endow P with the canonical *symplectic two-form*

$$\Omega=dq_1\wedge dp_1+\cdots+dq_N\wedge dp_N. \tag{49}$$

Then, pairs (P,Ω) and (P_μ,Ω_μ) define symplectic manifolds, where the reduced symplectic form Ω_μ is determined by the *Symplectic Reduced Theorem* [17]. For systems with Abelian symmetries, Ω_μ

DOI: 10.1002/nme

carries the canonical symplectic structure modified by magnetic terms β_μ. In particular, reductions with respect to translations given by the map $\pi(q)$, (37)–(38), induce the following *reduced symplectic two-form*

$$\Omega_{\mu_1} = \Omega - \beta_{\mu_1} = q'_1 \wedge dp'_1 + \cdots + dq'_{N-1} \wedge dp'_{N-1}, \tag{50}$$

where $p'_i = m'_i \dot{q}'_i$ and β_{μ_1} is the curvature of the mechanical connection, i.e. $\beta_{\mu_1} = dR \wedge d\mu_1$.

We recall (cf. e.g. [24–26]) that a diffeomorphism $\varphi : P \to P$ is *symplectic* if it preserves the symplectic two-form, i.e. if

$$\Omega(T\varphi(z)\eta_1, T\varphi(z)\eta_2) = \Omega(\eta_1, \eta_2). \tag{51}$$

Likewise, in reduced phase space, a diffeomorphism $\varphi : P_\mu \to P_\mu$ is symplectic if it preserves the reduced symplectic two-form. The symplecticity of Lipschitz homeomorphisms has been investigated by Whitney [27] and by Gol'dshtein and Dubrovskiy [28]. Then, in the present setting, it is possible to verify the symplecticity of force-stepping directly. To this end, we may write $\varphi(q'_0, p'_0) = (q'(t), p'(t))$ and

$$T\varphi \equiv \begin{pmatrix} \partial_{q'}\varphi_{q'} & \partial_{p'}\varphi_{q'} \\ \partial_{q'}\varphi_{p'} & \partial_{p'}\varphi_{p'} \end{pmatrix} = \begin{pmatrix} Q_{q'} & Q_{p'} \\ P_{q'} & P_{p'} \end{pmatrix}, \tag{52}$$

then φ is symplectic if

$$P_{p'}^{\mathrm{T}} Q_{p'} = Q_{p'}^{\mathrm{T}} P_{p'}, \tag{53}$$

$$P_{p'}^{\mathrm{T}} Q_{q'} = Q_{p'}^{\mathrm{T}} P_{q'} + I, \tag{54}$$

$$Q_{q'}^{\mathrm{T}} P_{q'} = P_{q'}^{\mathrm{T}} Q_{q'}. \tag{55}$$

We proceed to verify that these identities are indeed identically satisfied by the force-stepping scheme. For simplicity of notation and without loss of generality we take the mass matrix to be of the form $M = mI$. In addition, it suffices to consider mappings defined by the trajectory depicted in Figure 2, the general result then following by recursion. Evidently, the symplectic form is trivially conserved for $t \in [t_0, t_1)$, where t_1 is the time of intersection with the boundary of the underlying triangulation. For $t \in (t_1, t_2)$, the dependence of t_1 on the initial conditions $(\dot{q}_0, q_0)$ must be carefully accounted for, i.e.

$$\frac{\partial t_1}{\partial \dot{q}_0} = (t_1 - t_0)\frac{\partial t_1}{\partial q_0} = -\frac{t_1 - t_0}{\dot{q}(t_1)\cdot n} n = -\left|\frac{\partial t_1}{\partial \dot{q}_0}\right| n. \tag{56}$$

For $t \in (t_1, t_2)$ we have

$$\dot{q}(q_0, \dot{q}_0, t) = \dot{q}_0 - \frac{t_1 - t_0}{m}\nabla V_I - \frac{t - t_1}{m}\nabla V_{II}, \tag{57}$$

$$q(q_0, \dot{q}_0, t) = q_0 + (t - t_0)\dot{q}_0 - \frac{(2t - t_1 - t_0)(t_1 - t_0)}{2m}\nabla V_I - \frac{(t - t_1)^2}{2m}\nabla V_{II}. \tag{58}$$

DOI: 10.1002/nme

From these identities, the components of the Jacobian matrix $T\varphi$ are found to be

$$P_p = I - \frac{1}{m}|\nabla V_{II} - \nabla V_I| \left| \frac{\partial t_1}{\partial \dot{q}_0} \right| n \otimes n, \tag{59}$$

$$Q_p = (t - t_0)I - \frac{t - t_1}{m}|\nabla V_{II} - \nabla V_I| \left| \frac{\partial t_1}{\partial \dot{q}_0} \right| n \otimes n, \tag{60}$$

$$P_q = -\frac{1}{m}|\nabla V_{II} - \nabla V_I| \left| \frac{\partial t_1}{\partial q_0} \right| n \otimes n, \tag{61}$$

$$Q_q = I - \frac{t - t_1}{m}|\nabla V_{II} - \nabla V_I| \left| \frac{\partial t_1}{\partial q_0} \right| n \otimes n, \tag{62}$$

where the following identity has been used

$$\nabla V_{II} - \nabla V_I = \pm |\nabla V_{II} - \nabla V_I| n. \tag{63}$$

A straightforward calculation shows that the symplecticity relations (53) are identically satisfied by (59), (60), (61), and (62), which establishes the symplecticity of the force-stepping scheme.

4.5. Summary of the conservation properties of the force-stepping scheme

The results proven in the foregoing can be summarized as follows:

> *The force-stepping time-integration scheme is a symplectic, energy conserving, time-reversible integrator with automatic selection of the time-step size. The scheme also conserves approximately all the momentum maps associated with the symmetries of the system. Exact conservation of momentum maps may be achieved by recourse to Lagrangian reduction.*

Time-reversibility and parity-invariance of force-stepping follow directly from the definition of the scheme. The automatic time-step selection property also follows by construction. In particular, in regions where the velocity is high, the times effectively spent by the trajectory inside a simplex are short and the resulting time steps are small. In contrast, if the velocity is low, the resulting time steps are comparatively large.

Theorems 5.2 and 4.2 show that the naïve force-stepping scheme, while not exactly conserving in general, results in approximate momentum conservation, with the conservation error controlled uniformly on compact time intervals by the asymmetry of the approximate Lagrangian. This near-conservation property is frequently sufficient in applications and is borne out by the numerical examples presented in Section 6.

We again emphasize that the momentum maps that are nearly conserved by force-stepping are precisely those conserved by the original system. This is in contrast to variational integrators, which conserve discrete momentum maps that are a discretization of—and differ from in general—the momentum maps of the original system.

5. CONVERGENCE ANALYSIS

Assume that the configuration space is $\mathbb{R}^d$ and the potential $V : \mathbb{R}^d \to \mathbb{R}$ is a C^1 function bounded from below. We use a regular triangulation $\mathscr{T}_h$ of $\mathbb{R}^d$ (see Section 3) and define V_h as the

DOI: 10.1002/nme

corresponding continuous piecewise affine approximation of V. Clearly, $V_h \to V$ uniformly on compact subsets of $\mathbb{R}^d$.

The approximating trajectories q_h can be represented by their successive times of element boundary crossings $0=t_0<t_1<t_2<\dots$ and the corresponding sequences of positions $q_h(0), q_h(t_1), q_h(t_2), \dots$ and velocities $\dot{q}_h(0), \dot{q}_h(t_1), \dot{q}_h(t_2), \dots$. Note that the trajectories for the piecewise-linear continuous approximation are defined unambiguously as long as they are never tangential to the boundary of any cell of the underlying triangulation while crossing this boundary. We will call trajectories such that, for every k, $\dot{q}_h(t_k)$ is not aligned with F, where F is a face of a triangulation element such that $q_h(t_k) \in F$, *transversal*. If q is non-transversal we denote by $t_{\max}$ the first time t for which $q(t)$ lies on an element boundary and $\dot{q}(t)$ is aligned with that boundary.

We also have to make sure that our iterative procedure defines an approximate trajectory for all positive times. This does not follow from transversality as the sequence (t_k) could be bounded. If this is indeed the case, we define $t_{\max} := \lim_{k\to\infty} t_k \in \mathbb{R}$, and our approximate trajectory will be defined only on $[0, t_{\max})$. For transversal trajectories with $t_k \to \infty$ as $k \to \infty$ we set $t_{\max} = \infty$.

The main goal of this section will be to justify our approximation scheme by proving that—except for a negligibly small set of initial conditions—the approximating trajectories converge to the original trajectory in a rather strong sense along any sequence of triangulation parameters h tending to zero. More precisely, the exceptional set is shown to be of Hausdorff dimension at most $2d-1$ in the $2d$-dimensional phase space (and consequently its Lebesgue measure vanishes).

By construction, an approximating trajectory q_h lies in $C^1([0, t_{\max}))$ and satisfies

$$M\ddot{q} = -\nabla V_h(q) \quad \text{on } (0, t_{\max}) \tag{64}$$

for all times t such that $q(t)$ lies in the interior of some triangulation element. As an immediate consequence we obtain that q_h conserves energy:

Lemma 5.1
If q_h is an approximating trajectory with initial conditions $(q_0, \dot{q}_0)$, then

$$\tfrac{1}{2}\dot{q}_h^{\mathrm{T}}(t) M \dot{q}_h(t) + V_h(q_h(t)) = \tfrac{1}{2}\dot{q}_0^{\mathrm{T}} M \dot{q}_0 + V_h(q_0)$$

for all $t \in [0, t_{\max})$.

Proof
If $t \in [t_k, t_{k+1}]$, then

$$\tfrac{1}{2}\dot{q}_h^{\mathrm{T}}(t) M \dot{q}_h(t) + V_h(q_h(t)) = \tfrac{1}{2}\dot{q}_h^{\mathrm{T}}(t_k) M \dot{q}_h(t_k) + V_h(q_h(t_k))$$

since q_h is a solution of the Euler–Lagrange equation (64) on $[t_k, t_{k+1}]$. The claim now follows by induction on n. □

The approximating trajectories, being smooth inside the cells (a quadratic function) and C^1 across element boundaries, in fact belong to the Sobolev class $W^{2,\infty}_{\mathrm{loc}}([0, t_{\max}))$ of twice weakly differentiable functions whose second derivative is bounded on any compact time interval. More

DOI: 10.1002/nme

precisely, we have the following

Lemma 5.2
Approximating trajectories q_h are elements of $W^{2,\infty}_{\mathrm{loc}}([0,\infty))$ if $t_{\max}=\infty$. If $t_{\max}<\infty$, then $q_h \in W^{2,\infty}([0,t_{\max}])$. Moreover, if $(q_h)_{h>0}$ is a family of approximating trajectories with the same initial conditions, then, for each finite $T \leqslant t_{\max}$, $\|q_h\|_{W^{2,\infty}([0,T])}$ is equi-bounded in h.

Proof
Indeed, by Lemma 5.1 and the fact that V, and hence V_h, is bounded from below, $\dot{q}_h(t)$ is bounded uniformly in h and t and therefore $q_h(t)$ is bounded uniformly in h and uniformly in t on finite time intervals. But then also $\ddot{q}_h$ is bounded uniformly on finite time intervals as q_h satisfies (64) for almost all $t \in [0,t_{\max})$. In particular, if $t_{\max}<\infty$, then $\dot{q}_h$ can be extended as a Lipschitz function to $[0,t_{\max}]$. □

For purposes of analysis, it is useful to note that in fact any non-transversal trajectory satisfies the Euler–Lagrange equation in the weak sense:

Proposition 5.1
Suppose $t \mapsto q_h(t)$ is an approximating trajectory. Then (64) is satisfied in the weak sense, i.e. $\ddot{q}$ is the (piecewise continuous) weak second derivative of q and the equality is understood as equality almost everywhere on $(0,t_{\max})$.

Proof
This follows from the proof of Lemma 5.2: As q_h lies in $C^1([(0,t_{\max}))$, $\ddot{q}$ is piecewise continuous with only finitely many jumps on any compact interval in $(0,t_{\max})$ and q_h satisfies (64) for all times $t \notin \{t_0,t_1,t_2,\ldots\}$, (64) is easily seen to hold in the sense of distributions. □

Restricting our attention to transversal trajectories is justified by the following result.

Lemma 5.3
Let $h>0$. The set of initial conditions $(q_0,\dot{q}_0)$ for which the trajectory $(q_h(t),\dot{q}_h(t))$ is non-transversal has Hausdorff-dimension $2d-1$.

Proof
We first consider a single step $(q_{k-1},\dot{q}_{k-1}) \to (q_k,\dot{q}_k)$ of the dynamics: Let $\partial\mathscr{T}_h$ be the collection of element boundaries and define the mapping $\tau : \partial\mathscr{T}_h \times \mathbb{R}^d \to \partial\mathscr{T}_h \times \mathbb{R}^d$ in the following way: For $(q,\dot{q}) \in \partial\mathscr{T}_h \times \mathbb{R}^d$ solve the Euler–Lagrange equation (64) backwards in time with initial condition $(q,\dot{q})$ and define $\tau(q,\dot{q})$ to be the position and velocity at the first element boundary crossing. This is a well-defined mapping as long as $\dot{q}$ is not aligned with the boundary q lies on. In the exceptional case that $\dot{q}$ is aligned with this boundary we will view τ as being multivalued, more precisely $\tau(q,\dot{q})$ consisting of the set of transversal points in phase space $(\tilde{q},\dot{\tilde{q}})$ that are mapped to $(q,\dot{q})$ under the discrete dynamics. (Note that $\#\tau(q,\dot{q})$ is bounded by the number of elements incident to $(q,\dot{q})$.)

Fix $T>0$. Then on the set of those $(q,\dot{q})$ for which $\tau(q,\dot{q})$ is reached in a time span less than or equal to T, the mapping τ is locally Lipschitz. As the set of non-transversal points $(q,\dot{q})$, i.e. for which q lies on some element boundary and $\dot{q}$ is parallel to this boundary, is $(2d-2)$-dimensional, this proves that, for fixed $k \in \mathbb{N}$, the set of points $(q_1,\dot{q}_1)$ for which the corresponding trajectories satisfy $t_k \leqslant T$ and q_h is non-transversal at t_k is locally of finite $(2d-2)$-dimensional Hausdorff measure.

DOI: 10.1002/nme

Now note that clearly the pre-images of the mapping $(q_0, \dot{q}_0) \mapsto (q_1, \dot{q}_1)$ are of finite one-dimensional Hausdorff measure on the set of those $(q_0, \dot{q}_0)$ for which $t_1 \leqslant T$. Now finally sending $k \to \infty$ and $T \to \infty$, we obtain that the set of initial conditions for which t_k is non-transversal for some k is $(2d-1)$-dimensional. □

We also need to show that the set of trajectories with $t_{\max} < \infty$ is negligible in a suitable sense. Note first that our approximating trajectories—being elements of $W^{2,\infty}(0, t_{\max})$—can be extended to functions in $C^1([0, t_{\max}])$. To this end, we introduce the following two subsets of $\mathbb{R}^d$: By Δ_1 denote the set of all vectors in $\mathbb{R}^d$ which are aligned with some triangulation element face. As we use regular triangulations (see Section 3), Δ_1 is a $(d-1)$-dimensional set (the union of a finite number of hyperplanes) in $\mathbb{R}^d$. Similarly, let Δ_2 denote the set of vectors which are aligned with two non-parallel faces of some triangulation element. Then Δ_2 is a finite union of codimension 2 subspaces of $\mathbb{R}^d$, and in particular Δ_2 is $(d-2)$-dimensional.

Lemma 5.4
Suppose q_h is transversal. If $t_{\max} < \infty$, then necessarily $\dot{q}_h(t_{\max}) \in \Delta_2$.

Proof
If $t_{\max} < \infty$, then $t_k \to t_{\max}$ and there are infinitely many boundary crossing times t_{k_m}, say, at which the points $q_h(t_{k_m})$ lie on the same face F of a single triangulation element. We can decompose the particle motion $q_h = q_h^{F_\perp} + q_h^F$ into a scalar part $q_h^{F_\perp}$ perpendicular to F and a $(d-1)$-dimensional motion q_h^F parallel to F. Denote the two closed elements adjacent to F by F^+ and F^-.

We first show that $q_h(t_{\max})$ cannot lie in the interior of F. Suppose the contrary were true. As $t_{k_{m+1}} - t_{k_m} \to 0$ and the boundary $\partial(F^+ \cup F^-)$ of $(F^+ \cup F^-)$ is a positive distance apart from $q_h(t_{\max})$, for sufficiently large m, q_h cannot cross this boundary in between two crossings of F. Otherwise the transversal velocity $\dot{q}_h^{F_\perp}$ would diverge. It follows that, for t large enough, $q_h(t)$ alternates between F^+ and F^-. But then the explicit form of $q_h^{F_\perp}$ as a parabola shows that the time that elapses between two crossings of F can only take two different values (depending on wether the particle moves through F^+ or F^-) and in particular does not converge to zero. This contradicts the convergence of (t_k).

Thus we may assume that $q_h(t_{\max}) \in \partial F$. As we have just seen that q_h cannot lie in the interior of $F^+ \cup F^-$ for all times close to $t_{\max}$, we thus get another sequence $t_{k'_m}$ such that $q_h(t_{k'_m}) \in G$, where G is another face of F^+ or F^- such that $q_h(t_{\max}) \in \partial G$.

Note that the vector $q_h(t_{k_{m+1}}) - q_h(t_{k_m})$, and thus also the difference quotient $((q_h(t_{k_{m+1}}) - q_h(t_{k_m})))/(t_{k_{m+1}} - t_{k_m})$ is aligned with F. Taking the limit $m \to \infty$ we deduce that $\dot{q}_h^{F_\perp}(t_{\max}) = 0$, i.e. that also $\dot{q}_h(t_{\max})$ is aligned with this element face, since $q_h \in C^1([0, t_{\max}])$. An analogous argument with F replaced by G shows that $\dot{q}_h(t_{\max})$ is aligned with G, too. Thus in fact $\dot{q}_h(t_{\max})$ is aligned with $F \cap G$, and this concludes the proof. □

Before we prove convergence of the approximating trajectories, let us note that, for transversal initial conditions, the trajectories remain transversal for a non-zero time span independent of h.

Lemma 5.5
Suppose $\dot{q}_0 \notin \Delta_1$. Then there exists $T > 0$ independent of h such that $t_{\max}(h) > T$ for all h.

DOI: 10.1002/nme

Proof
As $\ddot{q}_h(t)$ is bounded independently of h on compact intervals by Lemma 5.2, by choosing T small enough, we may assume that $|\dot{q}_h(t)-\dot{q}_0|$ is so small that $\dot{q}_h(t)\notin\Delta_1$ for all $t\leqslant\min\{T, t_{\max}(h)\}$. But then q_h is transversal on $[0,\min\{T, t_{\max}(h)\}]$, and in particular $t_{\max}(h)>T$. The claim now follows. □

As a consequence, for transversal initial conditions this implies $\liminf_{h\to 0} t_{\max}(h)>0$.

Theorem 5.1
Fix initial conditions $(q_0,\dot{q}_0)$ such that $\dot{q}_0\notin\Delta_1$. For all $0<T<\liminf_{h\to 0} t_{\max}(h)$, the approximating trajectories q_h converge to the continuum trajectory q strongly in $W^{2,\infty}([0,T])$.

Proof
By Lemma 5.2 $\|q_h\|_{W^{2,\infty}([0,T])}$ is bounded independently of h. Passing—if necessary—to a subsequence, we may assume that $q_h \rightharpoonup^* q$ in $W^{2,\infty}([0,T])$ for some $q\in W^{2,\infty}([0,T])$. But then q_h converges strongly in $W^{1,\infty}$ by the Rellich compactness theorem and since $\nabla V_h\to\nabla V$ uniformly on compacts, we may pass to the limit in (64) to obtain that

$$M\ddot{q}=-\nabla V(q) \quad \text{on } [0,T].$$

As the right-hand side of (64) converges uniformly, also $\ddot{q}_h$ converges uniformly to $\ddot{q}$ and we obtain $q_h\to q$ strongly in $W^{2,\infty}([0,T])$.

Applying the above reasoning to an arbitrary subsequence $h_m\to 0$, we have thus proved that a further subsequence converges to a solution q of the original equation of motion. As this solution is unique, indeed the family q_h converges to q. □

We are now in a position to state and prove our main global convergence result. In Lemma 5.3 we have seen that the element boundary crossings of approximating sequences are transversal except for a $(2d-1)$-dimensional set of initial conditions. This exceptional set does indeed depend on h and, therefore, if h is viewed as a real variable we cannot expect that the set of exceptional initial values can be chosen negligibly small independently of h. However, in practice this problem does not occur since every numerical scheme is restricted to sequences $h_m\to 0$. Under these conditions, the following theorem shows that the exceptional set is indeed negligible.

Theorem 5.2
Let $h_m\to 0$. Then except for a $(2d-1)$-dimensional set of initial conditions $(q_0,\dot{q}_0)$, q_{h_m} converges to the continuum solution q strongly in $W^{2,\infty}_{\mathrm{loc}}([0,\infty))$.

Proof
As $\{h_m\}$ is countable, by Lemma 5.3 we may assume that all the element boundary crossings at times $t_1(h_m), t_2(h_m), \ldots$ are transversal. By Theorem 5.1 it suffices to show that $\liminf_{m\to\infty} t_{\max}(h_m)=\infty$. Suppose this were not the case, say $\liminf_{m\to\infty} t_{\max}(h_m)=\bar{t}<\infty$. By passing to a subsequence (not relabeled) we may assume that $\bar{t}=\lim_{m\to\infty} t_{\max}(h_m)$. Now Lemma 5.4 implies that $\dot{q}_{h_m}(t_{\max}(h_m))\in\Delta_2$. On the other hand, we deduce from Theorem 5.1 that, for all $T<\bar{t}$, $\dot{q}_{h_m}(T)\to\dot{q}(T)$. As by Lemma 5.2 $\sup_{[T,t_{\max}]}\ddot{q}_{h_m}(t)$ is uniformly bounded, Δ_2 is closed and $\dot{q}$ is continuous, sending $T\to\bar{t}$ we deduce that $\dot{q}(\bar{t})\in\Delta_2$. We conclude the proof by showing that the set of initial conditions for which $\dot{q}(t)\in\Delta_2$ at some positive time t has Hausdorff dimension $2d-1$: Let $\Phi\colon\mathbb{R}\times\mathbb{R}^d\times\mathbb{R}^d\to$

DOI: 10.1002/nme

$\mathbb{R}^d \times \mathbb{R}^d$ be the flow associated with the continuum equations of motion

$$\dot{q}(t) = p(t),$$
$$\dot{p}(t) = -M^{-1}\nabla V(q(t)),$$

i.e. solutions with initial conditions (q_0, p_0) are given by $(q(t), p(t)) = \Phi(t, q_0, p_0)$. The critical set of initial conditions under investigation is then given by

$$\bigcup_{t\in[0,\infty)} \Phi_t^{-1}(\mathbb{R}^d \times \Delta_2) = \Phi^{-1}(\mathbb{R}^d \times \Delta_2),$$

where $\Phi_t = \Phi(t, \cdot)$. As $(t, q, p) \mapsto (t, \Phi_t(q, p))$ is a diffeomorphism on $\mathbb{R}^{2d+1}$ and Δ_2 is $(d-2)$-dimensional, the set $\{(t, q_0, p_0) : (t, \Phi_t(q_0, p_0)) \in \mathbb{R} \times \mathbb{R}^d \times \Delta_2\}$ is $(2d-1)$-dimensional. But $\Phi^{-1}(\mathbb{R}^d \times \Delta_2)$ is just the projection onto the first coordinate of this set. As projections—being Lipschitz continuous—do not enlarge the dimension of a set, we have indeed $\dim \Phi^{-1}(\mathbb{R}^d \times \Delta_2) \leqslant 2d-1$. □

6. NUMERICAL EXAMPLES

We begin with the following quote from the survey of open problems in symplectic integration by McLachlan and Scovel [29]:

How efficient can symplectic integrators be, given only the Hamiltonian (Lagrangian) function?

The answer of this question is of practical relevance either when the Lagrangian is so complicated that one does not wish to calculate its derivative by hand or when the numerical evaluation of the derivative is so computationally demanding that one does not wish to use a time integrator that relies on its calculation, e.g. multiscale modeling of materials. The force-stepping integrator defined in Section 2 and the continuous piecewise-linear representation of approximate energies presented in Section 3 result in a time integration scheme which only requires one evaluation of the potential energy in each step. Thus, force-stepping could shed some light on the question posed above.

Next, we present selected examples of applications that showcase the conservation, accuracy, long-term behavior, and convergence properties of force-stepping. These properties play an important role in the long-term behavior of problems with strong non-linearities, e.g. long-term integration in celestial mechanics and computation of thermodynamics properties in molecular dynamics. For instance, experience has shown that time-step adaption provides an efficient way to cope with strong non-linearities, but it is also observed that it tends to degrade the long-term behavior of standard time integrators [30, 31]. We illustrate the performance of force-stepping in those areas of application by means of three examples: the motion of two bodies that attract each other by Newton's law of gravitation, that is the Kepler problem, the dynamics of a frozen argon cluster, and the oblique impact of an elastic cube. In the first example, we investigate Lagrangian reductions with respect to translational and rotational symmetries. In the second example, we only investigate translational symmetry reductions by means of the general procedure presented in Section 4. In the third example, we do not carry out any Lagrangian reduction.

For purposes of assessing the performance of force-stepping, we draw detailed comparisons with the second-order explicit Newmark method, namely, the member of the Newmark family of time-stepping algorithms corresponding to parameters $\beta = 0$ and $\gamma = 1/2$ (cf., e.g. [32] for a

DOI: 10.1002/nme

detailed account of Newmark's method). In the linear regime, explicit Newmark is second-order accurate and conditionally stable, with a critical time step equal to twice over the maximum natural frequency of the system. Explicit Newmark is identical to velocity Verlet and, for constant time step, it is also identical to central differences. It can also be shown that the Newmark solution is in one-to-one correspondence, or 'shadows', the solution of the trapezoidal-rule variational integrators (cf., e.g. [32]). Thus, explicit Newmark provides a convenient representative of a time integrator commonly used in molecular dynamics, finite-differencing, and variational integration.

Detailed analyses of the implicit members of the Newmark family of algorithms, their stability, and energy preserving properties (for linear systems) were given in Belytschko and Schoeberle [33], Hughes [34], and related papers.

6.1. Kepler problem

6.1.1. Lagrangian reduction. The motion of two bodies that attract each other by Newton's inverse square law of gravitation is often called the Kepler problem. This problem is characterized by a Lagrangian $L:\mathbb{R}^6\times\mathbb{R}^6\to\mathbb{R}$ of the form (1) and is rich in symmetries and constants of motion. Among these invariants, the total linear momentum and the total angular momentum are relevant to our analysis. We first apply the ideas of Lagrangian reduction, presented in Section 4, to reduce the dimension of phase space to $TQ=\mathbb{R}^2\times\mathbb{R}^2$. More precisely, we chose one of the bodies as the center of the coordinate system in order to have a two-dimensional motion $q=(x,y)$. Then, the Lagrangian reduces to

$$L(x,y,\dot{x},\dot{y})=\frac{1}{2}(\dot{x}^2+\dot{y}^2)+\frac{1}{\sqrt{x^2+y^2}}. \tag{65}$$

and the solution is stable and periodic for initial conditions of the family

$$q_0=(1-e,0),\quad \dot{q}_0=\left(0,\sqrt{\frac{1+e}{1-e}}\right) \tag{66}$$

with $0\leqslant e<1$. Indeed, Kepler's first law states that planets move in elliptic orbits with the sun at one of the foci.

It is possible to further reduce phase space by first changing the coordinates to a polar representation and then by eliminating the angular components, i.e. the group coordinates associated with the rotational symmetry. Then, reduction by stages gives a reduced Lagrangian $l:\mathbb{R}\times\mathbb{R}\to\mathbb{R}$ of the form (1),

$$l(r,\dot{r})=\tfrac{1}{2}\dot{r}^2-V'(r), \tag{67}$$

$$\theta(t)=\int_0^t\frac{\Theta}{r(\tau)^2}d\tau+\theta_0, \tag{68}$$

where the effective potential is $V'(r)=-1/r+\Theta^2/2r^2$, and the total angular momentum is $\Theta=r\dot{\theta}=x\dot{y}-y\dot{x}$. Initial conditions are

$$r_0=1-e,\quad \dot{r}_0=0,\quad \Theta=\sqrt{1-e^2},\quad \theta_0=0. \tag{69}$$

A unique property of 2-body problems, e.g. the Kepler problem, is that reduction with respect to translational and rotational symmetries induces Lagrangians of the desirable form (1). Therefore,

DOI: 10.1002/nme

force-stepping trajectories can be readily obtained either from (65) or from (67). The latter are linear and angular momenta preserving and the former are linear momentum preserving. This is in sharp contrast to N-body problems with $N \geqslant 3$, which only allow for an effective reduction with respect to the translational symmetry, as described in Section 4.

We first consider the Kepler problem described by the Lagrangian (65) and initial conditions (66) with $e=0.85$. The size of the underlying simplicial triangulation employed in the force-stepping calculations is $h_{x,y}=0.022$. The time step employed in the time-stepping calculations is $\Delta t=0.0125$, which corresponds to the average time step resulting from the force-stepping calculations. The total duration of the analysis is 64π.

The constant time-step explicit Newmark method is symplectic-momentum preserving and, therefore, does not conserve energy. As it is often the case with symplectic-momentum preserving methods, it nevertheless has good energy-conservation properties for sufficiently small time steps. However, due to the conditional stability of the method the time-step is constrained by the maximum natural frequency of the system. The one-step explicit algorithm is

$$q_{k+1} = q_k + \Delta t \dot{q}_k - \frac{\Delta t^2}{2} M^{-1} \nabla V(q_k),$$

$$\dot{q}_{k+1} = \dot{q}_k - \frac{\Delta t}{2} M^{-1} [\nabla V(q_k) + \nabla V(q_{k+1})].$$

By way of contrast, LaBudde and Greenspan [35] presented a second-order accurate and symmetric method which is energy-momentum preserving and, therefore, does not conserve the symplectic structure. This time integrator was designed as a modification of the midpoint rule method considering a potential energy of the form $V(q)=U(|q|)$, e.g. the Kepler problem satisfies this restrictive condition. The one-step implicit algorithm is

$$q_{k+1} = q_k + \frac{\Delta t}{2}(\dot{q}_k + \dot{q}_{k+1}),$$

$$\dot{q}_{k+1} = \dot{q}_k - \Delta t \frac{U(|q_{k+1}|) - U(|q_k|)}{|q_{k+1}|^2 - |q_k|^2} M^{-1}(q_{k+1} + q_k).$$

Figure 5 shows the trajectories provided by force-stepping, explicit Newmark, and the energy-momentum preserving time integrator. Although a precession effect is characteristic of these numerical trajectories, we note that orbits are stable and elliptic over long times. The good long-time behavior of force-stepping and explicit Newmark is due to their exact conservation of the symplectic structure. In contrast, the good long-time behavior of the energy-momentum method is understood as a consequence of its time-reversibility more than of its exact conservation properties [23]. Conservation of the total energy and/or the angular momentum of these methods is verified in Figure 6. It is also worth noting that, at least for this dynamic system of interest, there is no apparent *drift* in the angular momentum of force-stepping trajectories. This may be understood as a consequence of the near-momentum conservation properties of the method (Theorem 4.2).

Figure 7 shows a histogram of the time steps selected by force-stepping. The broad range of time steps is noteworthy, as is their distribution in configuration space shown on the right side of Figure 5. In regions where the velocity is high (low), the resulting time steps are small (large). Thus, these figures also illustrate the automatic time-selection property of force-stepping. This property may in turn be regarded as the means by which force-stepping achieves symplecticity, exact conservation of energy, and approximate conservation of momentum maps. It also

DOI: 10.1002/nme

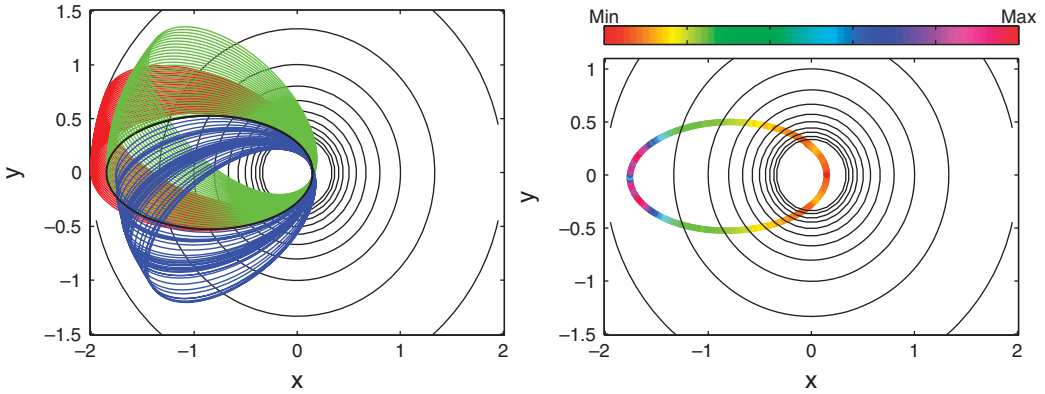

Figure 5. Kepler problem described by $L(x, y, \dot{x}, \dot{y})$ with $e = 0.85$ and $\Delta t = 0.0125$. Left: Force-stepping (blue line), Newmark (red line), energy-momentum (green line), and exact (black line) trajectories in configuration space. Right: Spatial distribution of time steps selected by force-stepping for $h_{x,y} = 0.022$.

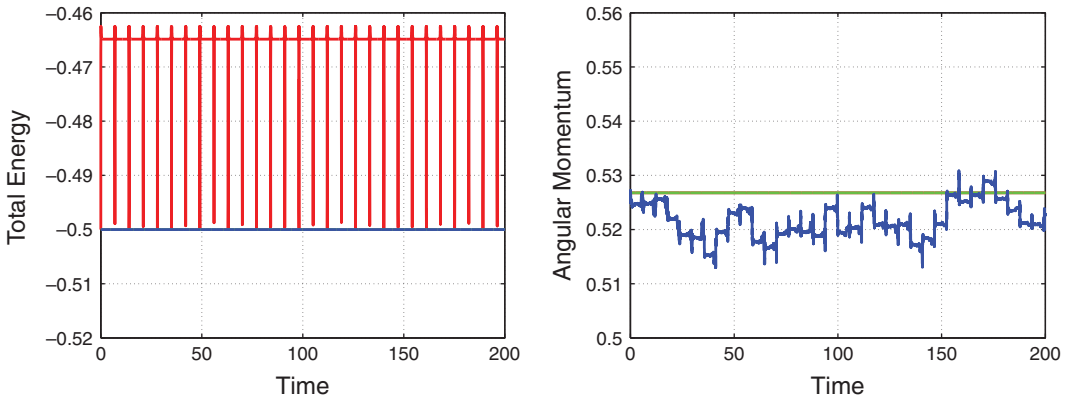

Figure 6. Kepler problem described by $L(x, y, \dot{x}, \dot{y})$ with $e = 0.85$. The force-stepping solution ($h_{x,y} = 0.022$) shows exact conservation of energy and near-conservation of momentum. The Newmark solution ($\Delta t = 0.0125$) shows near-conservation of energy and exact conservation of momentum. The time step employed in the energy-momentum calculations is $\Delta t = 0.0125$.

bears emphasis that, unlike variable time-step variational integrators designed to conserve energy [36, 37], force-stepping always selects a valid time step and is therefore free of solvability concerns.

We now consider the Kepler problem described by the reduced Lagrangian (67) and initial conditions (69) with $e = 0.85$. The size of the underlying simplicial triangulation employed in the force-stepping calculations is $h_r = 0.0067$—we note that the simplicial triangulation reduces to a one-dimensional grid. The time step employed in the time-stepping calculations is $\Delta t = 0.0125$, which corresponds to the average time step resulting from the force-stepping calculations as well as to the time step employed in the above calculations. The total duration of the analysis is 64π.

DOI: 10.1002/nme

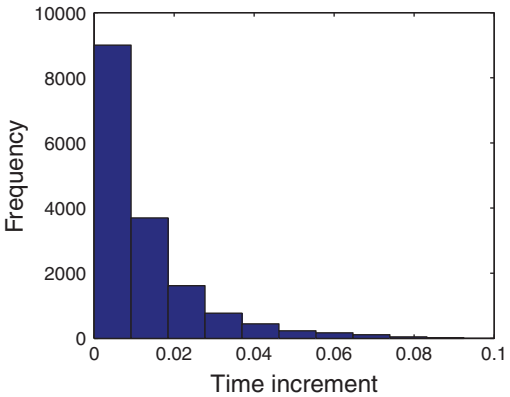

Figure 7. Kepler problem described by $L(x, y, \dot{x}, \dot{y})$ with $e = 0.85$. Histogram of time steps selected by force-stepping for $h_{x,y} = 0.022$.

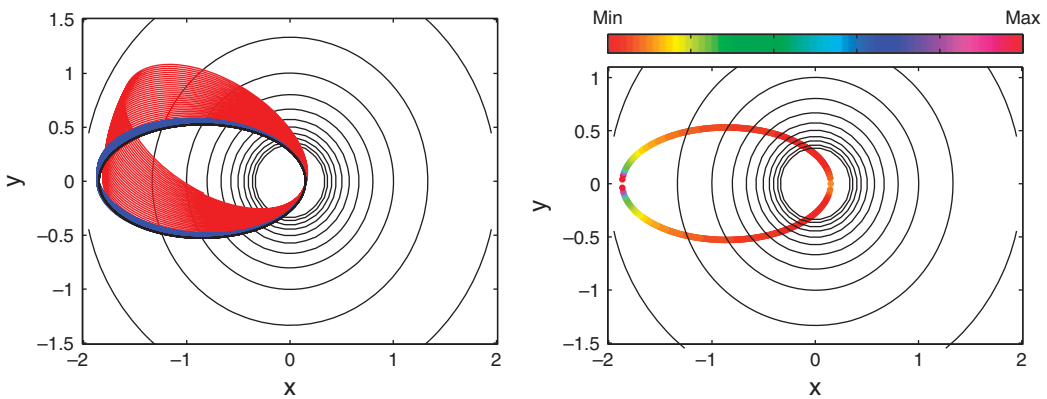

Figure 8. Kepler problem described by $l(r, \dot{r})$ with $e = 0.85$ and $\Delta t = 0.0125$. Left: Force-stepping (blue line), Newmark (red line) and exact (black line) reconstructed trajectories in configuration space. Right: Spatial distribution of time steps selected by force-stepping for $h_r = 0.0067$.

Figure 8 shows the reconstructed trajectories provided by force-stepping and explicit Newmark. The original dynamics is reconstructed from the reduced dynamics by computing $\theta(t)$ from (68). The angular displacement can be exactly obtained from force-stepping trajectories and therefore the total angular momentum map is conserved along the reconstructed trajectories. Conservation of the total energy and the angular momentum of the reconstructed trajectories is verified in Figure 9. As demonstrated in Section 4, force-stepping is a symplectic-energy time-reversible integrator which, by recourse to Lagrangian reduction, conserves exactly the total linear and angular momentum maps of the original Lagrangian.

It is suggestive to note that the automatic time-selection property of force-stepping leads to a sharper distribution of time steps in the reduced configuration space than in the original

DOI: 10.1002/nme

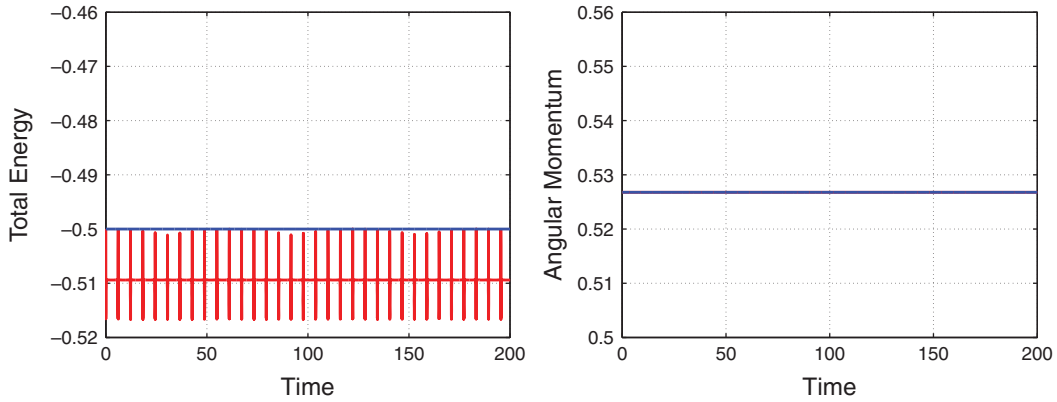

Figure 9. Kepler problem described by $l(r,\dot{r})$ with $e=0.85$. The force-stepping solution ($h_r=0.0067$) shows exact conservation of energy and momentum. The Newmark solution ($\Delta t=0.0125$) shows near–conservation of energy and exact conservation of momentum.

configuration space (cf. the right side of Figure 5 and the right side of Figure 8). The direct relationship between group symmetries of the system and optimal time-step adaption is noteworthy.

6.1.2. Strong non-linearities. McLachlan and Scovel [29] recognize the Kepler problem with $e\to 1$ as a strong non-linear problem and suggest taking this case as a good test of a variable time step method. We then consider the Kepler problem described by the Lagrangian (65) and initial conditions (66) with $e=0.99$. Thus, the potential energy gradient goes from $\nabla V(q_0)=(10^4,0)$ at the initial configuration to $\nabla V(q_a)\simeq(1,0)$ at the apoapsis—farthest point from the focus. The size of the underlying simplicial triangulation employed in the force-stepping calculations is $h_{x,y}=0.000247$. The time step employed in the time-stepping calculations is $\Delta t=0.000175$, which corresponds to the average time step resulting from the force-stepping calculations. The total duration of the analysis is 16π.

Figure 10 shows force-stepping, explicit Newmark, and energy-momentum preserving trajectories in configuration space. We first note that the orbits of both force-stepping and energy-momentum methods are stable and elliptic over long times, whereas explicit Newmark does not even exhibit the qualitative periodic behavior of the solution. We also note that a larger precession effect of the energy-momentum preserving integrator is in clear detriment of its pointwise accuracy. The remarkable behavior of force-stepping relays on its automatic time-step selection required for achieving symplecticity, exact conservation of energy, and approximate conservation of momentum maps. Indeed, the direct relationship between the spatial distribution of time steps and the non-linearity of the problem—visualized by the iso-curves of potential energy—is illustrated on the right side of Figure 10. In contrast, the good behavior of the energy-momentum method may relay on its implicit algorithm specially designed for central field forces, i.e. $V(q)=U(|q|)$, which is significantly more computationally expensive than force-stepping—force-stepping has complexity $O(d^2)$ whereas the energy-momentum method requires the solution of a non-linear system with complexity $O(d^3)$. Finally, conservation of the total energy and the angular momentum are verified in Figure 11.

DOI: 10.1002/nme

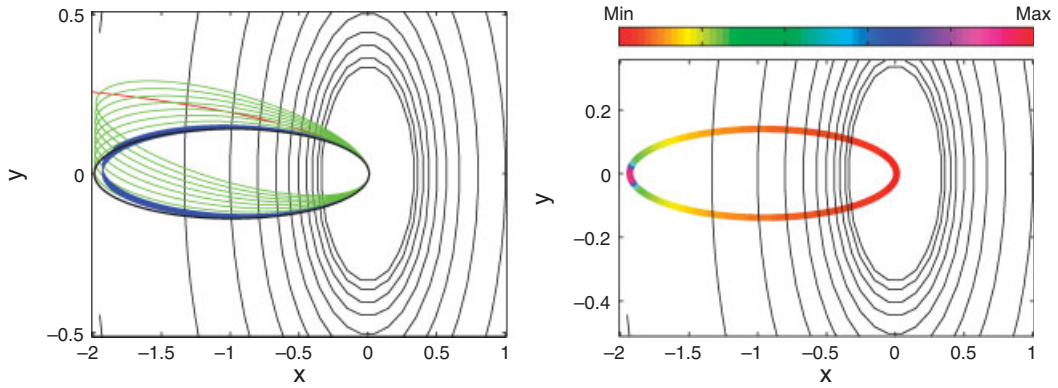

Figure 10. Kepler problem described by $L(x, y, \dot{x}, \dot{y})$ with $e = 0.99$ and $\Delta t = 0.000175$. Left: Force-stepping (blue line), Newmark (red line), energy-momentum (green line), and exact (black line) trajectories in configuration space. Right: Spatial distribution of time steps selected by force-stepping for $h_{x,y} = 0.000247$.

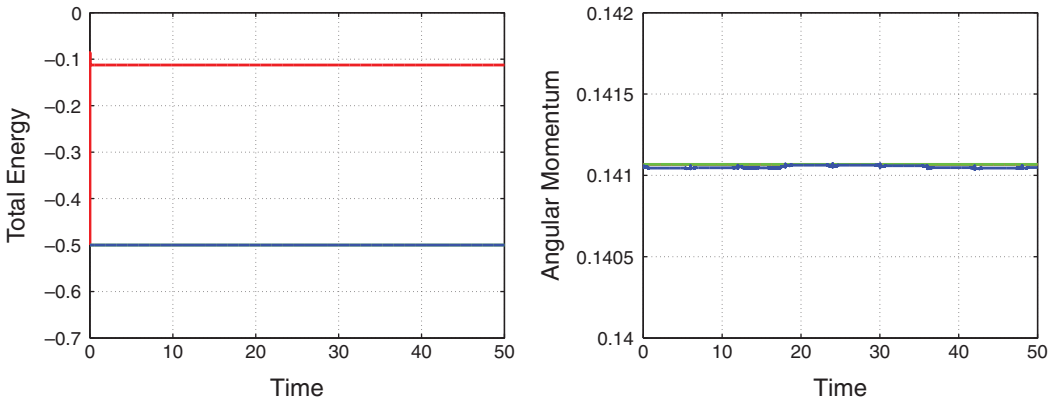

Figure 11. Kepler problem described by $L(x, y, \dot{x}, \dot{y})$ with $e = 0.99$. The force-stepping solution ($h_{x,y} = 0.000247$) shows exact conservation of energy and near-conservation of momentum. The Newmark solution ($\Delta t = 0.000175$) shows near-conservation of energy and exact conservation of momentum. The time step employed in the energy-momentum calculations is $\Delta t = 0.000175$.

6.1.3. Convergence analysis. We motivate this section with the following problem posed by McLachlan and Scovel [29]:

> *Develop variable time-step symplectic integrators so that they are competitive for pointwise accuracy with standard methods for the Kepler problem, while retaining the good long-time behavior of constant time-step symplectic methods.*

To this end, we first recall those characteristic parameters that describe the exact solution of the Kepler problem, i.e. the semi-major axis $a = L_0^2/(1-e^2) = 1$, the semi-minor axis $b = (1-e^2)^{1/2}$ and the period $\omega = 2\pi$. In the spirit of phase error analysis [34, 38, 39], these are the *statistical*

DOI: 10.1002/nme

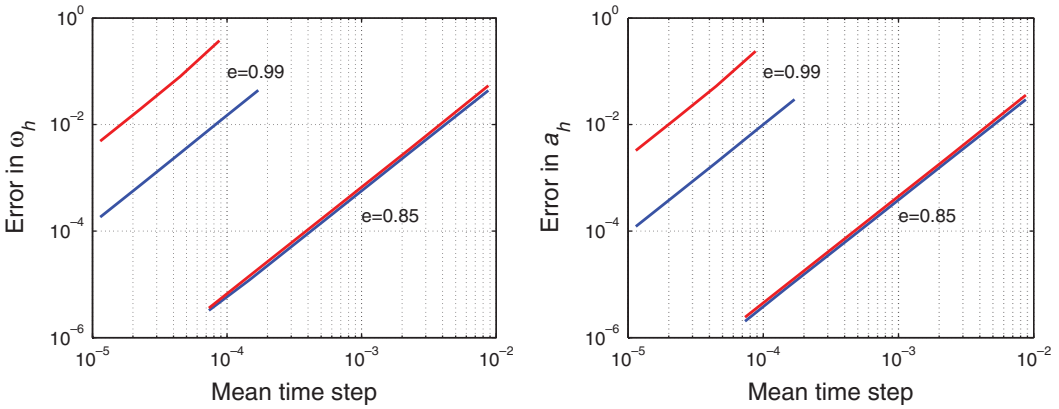

Figure 12. Kepler problem described by $L(x, y, \dot{x}, \dot{y})$ with $e=0.85$ and $e=0.99$. From left-top to bottom-right: 1st and 3rd curves correspond to Newmark solutions, 2nd and 4th curves correspond to force-stepping solutions.

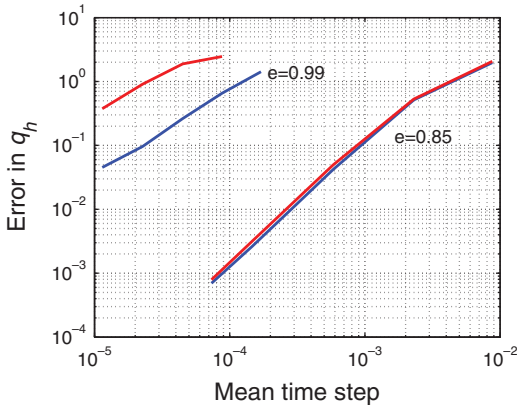

Figure 13. Kepler problem described by $L(x, y, \dot{x}, \dot{y})$ with $e=0.85$ and $e=0.99$. From left-top to bottom-right: 1st and 3rd curves correspond to Newmark solutions, 2nd and 4th curves correspond to force-stepping solutions.

quantities relevant to a global accuracy analysis rather than individual trajectories over intermediate to long time scales.

Figure 12 shows the convergence results for $a_h \to a=1$ and $\omega_h \to \omega=2\pi$, i.e. the *spectral convergence*. Figure 13 shows the convergence results for $|q_h - q|_\infty \to 0$, i.e. *pointwise convergence*. We note that the force-stepping is one order of magnitude more accurate than explicit Newmark when the problem has strong non-linearities ($e=0.99$). We also note that both methods have the same convergence rate and exhibit nearly identical accuracy characteristics when the problem has moderate non-linearities ($e=0.85$). These results not only indicate that standard time integrators, e.g. explicit Newmark, are particularly not efficient nor effective in solving problems with strong non-linearities during large periods of time, but they also demonstrate that force-stepping significantly outperforms the classical methods under these conditions.

DOI: 10.1002/nme

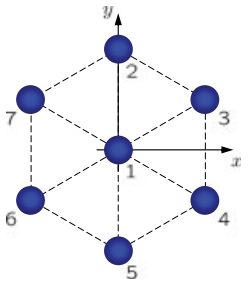

Figure 14. Frozen argon cluster.

Table I. Frozen argon cluster: initial conditions.

Atom	1	2	3	4	5	6	7
Position (nm)	0.00	0.02	0.34	0.36	−0.02	−0.35	−0.31
	0.00	0.39	0.17	−0.21	−0.40	−0.16	0.21
Velocity (nm/ns)	−30	50	−70	90	80	−40	−80
	−20	−90	−60	40	90	100	−60

6.2. *Frozen argon cluster*

Molecular dynamics falls squarely within the framework considered in this paper. Many applications in materials science, such as the calculation of free energies, require the integration of the system over long periods of time. In these applications, it is essential that the time integrators have good long-time behavior, such as conferred by symplecticity and exact conservation properties.

The velocity Verlet scheme is perhaps the most widely used time-integration scheme in molecular dynamics. As already noted, velocity Verlet is identical to explicit Newmark and, for constant time steps, it is symplectic-momentum preserving with good energy-conservation properties for sufficiently small time steps. However, due to the conditional stability of the method the time-step is constrained by the period of thermal vibrations of the atoms, which renders calculations of equilibrium thermodynamic properties exceedingly costly. The development of integration schemes that alleviate or entirely eliminate the time-step restrictions of explicit integration in molecular dynamics applications is the subject of ongoing research (cf., e.g. [40, 41]).

We proceed to illustrate the performance of force-stepping in molecular dynamics applications by analyzing the dynamics of a simple argon cluster. Specifically, we consider the numerical experiment proposed by Biesiadecki and Skeel [42]. The experiment concerns the two-dimensional simulation of a seven-atom argon cluster, six atoms of which are arranged symmetrically around the remaining central atom, Figure 14. The atoms interact via the pairwise Lennard-Jones potential

$$\phi(r)=4\varepsilon\left[\left(\frac{\sigma}{r}\right)^{12}-\left(\frac{\sigma}{r}\right)^{6}\right], \tag{70}$$

where r is the distance between two atomic centers, $\varepsilon/k_B=119.8\,\mathrm{K}$ and $\sigma=0.341\,\mathrm{nm}$ are material constants for Argon, and $k_B=1.380658\cdot10^{-23}\,\mathrm{J/K}$ is the Boltzmann's constant. In addition, the mass of an argon atom is $m=66.34\cdot10^{-27}\,\mathrm{kg}$. The initial positions of the atoms are slightly perturbed about the configuration that minimizes the potential energy of the cluster. The initial velocities are chosen such that the total linear momentum is zero and the center of mass of the

DOI: 10.1002/nme

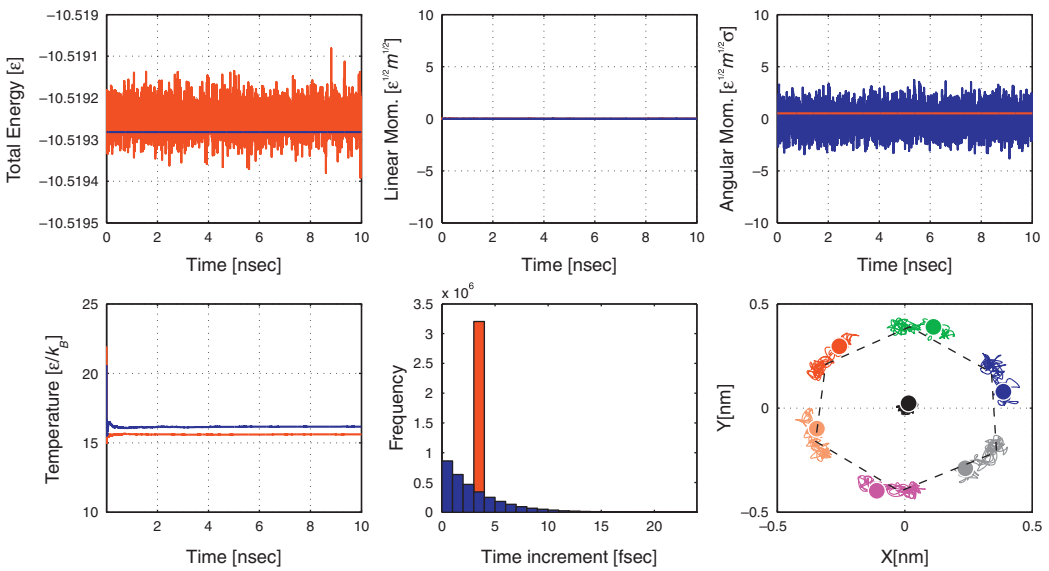

Figure 15. Frozen argon cluster. Blue line: Force-stepping solution with $h_1 = 0.02$ nm. Red line: Newmark solution with $\Delta t_1 = 3.12$ fs.

cluster remains fixed. The corresponding total energy of the cluster is $E/\varepsilon = -10.51928$. Table I summarizes the initial conditions for the simulation.

Two different discretizations of configuration space are employed in the force-stepping calculations: $h_1 = 0.020$ and $h_2 = 0.005$ nm. The time steps employed in the velocity Verlet calculations are $\Delta t_1 = 3.12$ fs and $\Delta t_2 = 0.80$ fs. These time steps correspond to the average time steps resulting from the respective force-stepping calculations. The total duration of the analysis is 10 ns.

The first row of Figures 15 and 16 shows the evolution in time of the constants of motion of the system: (i) total energy, (ii) total linear momentum, and (iii) total angular momentum. As expected, force-stepping is energy and linear momentum preserving regardless the discretization of configuration space employed. It is worth noting that, while not being exactly angular momentum conserving, force-stepping exhibits good angular momentum behavior over long times.

In order to assess the long-time behavior of force-stepping, we present on the second row of Figures 15 and 16 the qualitative behavior of the trajectories: (iv) the evolution in time of the numerical temperature of the cluster, (v) a histogram of time steps selected by the time integrator, and (vi) the trajectories of the argon atoms for a time window of [9.95, 10] nanosecond (the configuration at $t = 0$ is represented by the dashed line hexagon). The numerical temperature of the cluster is computed, under the assumption of ergodicity, by

$$T(t) = \frac{1}{tNk_B} \int_0^t \frac{1}{2} m \|\dot{q}(\tau)\|^2 \mathrm{d}\tau, \tag{71}$$

where $N = 7$ is the number of particles of the cluster. We note that force-stepping does not suffer from numerical dissipation and the system quickly reaches a thermodynamic temperature—the thermodynamic temperature is defined in the limit of $t \to \infty$. We also note that trajectories of the seven argon atoms, each represented by a different color, remain stable over long periods of time.

DOI: 10.1002/nme

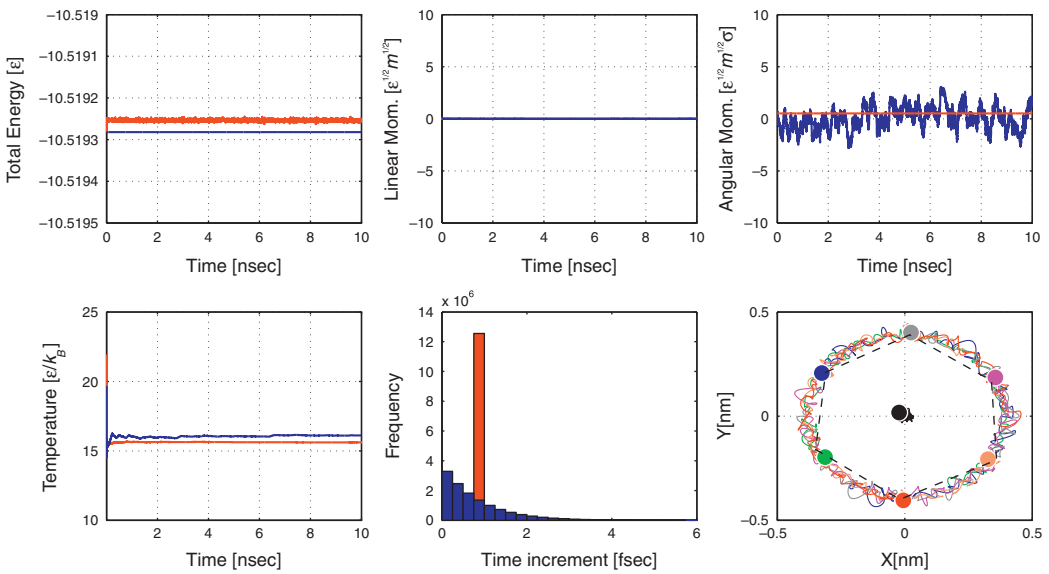

Figure 16. Frozen argon cluster. Blue line: Force-stepping solution with $h_2 = 0.005\,\text{nm}$. Red line: Newmark solution with $\Delta t_2 = 0.80\,\text{fs}$.

Finally, the convergence statement of Theorem 5.2 is illustrated by Figures 17 and 18. We first recall that, as demonstrated in Section 5, the approximate space of trajectories is $X = W^{2,\infty}_{\text{loc}}(0,T)$. Then, distances are measured with respect to the $W^{2,\infty}$-norm

$$\|q\|_{W^{2,\infty}(0,T)} = \|q(t)\|_{L^\infty} + \|\dot{q}(t)\|_{L^\infty} + \|\ddot{q}(t)\|_{L^\infty}, \tag{72}$$

and a relative $W^{2,\infty}$-error is defined by

$$W^{2,\infty}-\text{error} = \frac{|\,\|q_h\|_{W^{2,\infty}(0,T)} - \|q\|_{W^{2,\infty}(0,T)}|}{\|q\|_{W^{2,\infty}(0,T)}}, \tag{73}$$

where $\|q\|_{W^{2,\infty}(0,T)}$ is estimated from the numerical results. The relative $W^{2,\infty}$-error of force-stepping with and without parity-invariance is shown on the right side of Figures 17 and 18, respectively, as a function of the simplicial grid size h, for $T = 0.1\,\text{ns}$. The slope of the convergence plot is also directly related to the rate of convergence in grid size, which is $W^{2,\infty}\text{-error} = O(h^r)$. This gives an estimated rate of convergence in the $W^{2,\infty}$-norm of $r \simeq 1$. Furthermore, it is interesting to observe on the left side of Figures 17 and 18 that the average and the maximum time steps selected by force-stepping are $O(h)$. Additionally, the minimum time step selected by the method is $O(h^{7/4})$ when an approximate potential V_h with parity-invariance is employed, and $O(h^2)$ when the approximate potential breaks the parity symmetry of the exact potential V. It is also interesting to note that force-stepping with parity-invariance exhibits a region of asymptotic convergence larger than force-stepping without parity-invariance. Therefore, the sequence q_h is indeed convergent and transversal, as expected from the analysis in Section 5, and force-stepping with parity-invariance exhibits better convergence properties.

DOI: 10.1002/nme

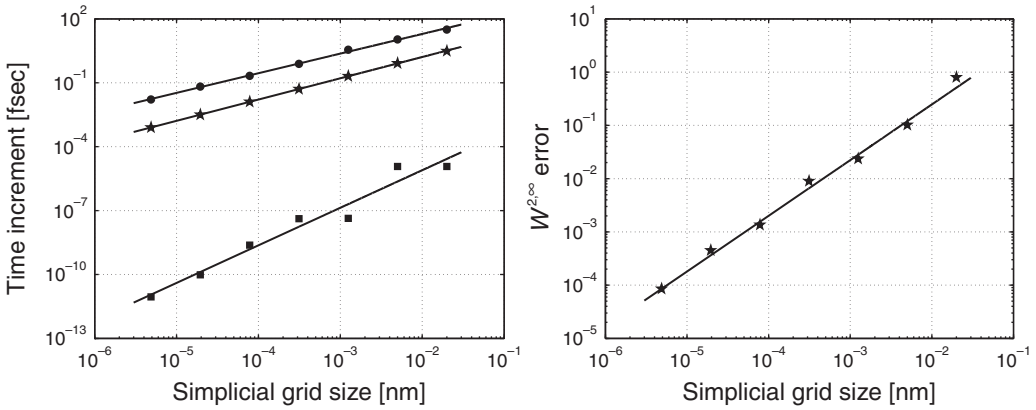

Figure 17. Convergence analysis of the frozen argon cluster using force-stepping with parity-invariance. Right: Convergence is observed in the $W^{2,\infty}$-norm with estimated convergence rate of $r \simeq 1$. Left: The average ($\star$) and the maximum ($\bullet$) time steps selected by force-stepping are $O(h)$, whereas the minimum ($\blacksquare$) time step is $O(h^{7/4})$.

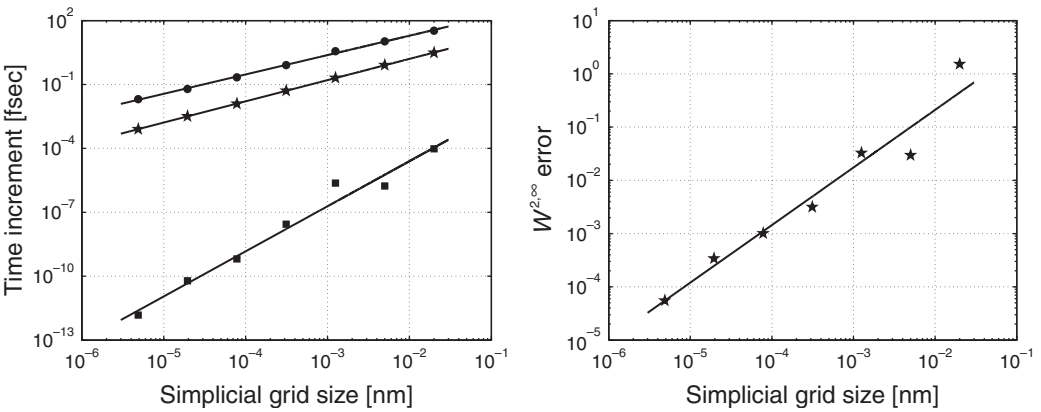

Figure 18. Convergence analysis of the frozen argon cluster using force-stepping without parity-invariance. Right: Convergence is observed in the $W^{2,\infty}$-norm with estimated convergence rate of $r \simeq 1$. Left: The average ($\star$) and the maximum ($\bullet$) time steps selected by force-stepping are $O(h)$, whereas the minimum ($\blacksquare$) time step is $O(h^2)$.

6.3. Finite-element model with contact: oblique impact of neo-Hookean cube

Next we consider finite-dimensional Lagrangian systems obtained by a finite-element discretization of the action of a non-linear elastic solid (cf., e.g. [37] for details of finite-element approximation in elastodynamics). For these applications, the generalized coordinates q of the system are the coordinates of the nodes in the deformed configuration of the solid. The example that we present

DOI: 10.1002/nme

to illustrate the performance of force-stepping in that area of application is the oblique impact of a neo-Hookean cube in a rigid wall. To this end, we assume a strain-energy density of the form

$$W(F)=\frac{\lambda_0}{2}(\log J)^2-\mu_0\log J+\frac{\mu_0}{2}\ \mathrm{tr}\ (F^{\mathrm{T}}F), \tag{74}$$

which describes a neo-Hookean solid extended to the compressible range. In this expression, λ_0 and μ_0 are Lamé constants, and J is the Jacobian of the deformation gradient F.

In problems involving contact we additionally consider the kinematic restrictions imposed by the impenetrability constraint. We recall that the admissible configuration set $\mathscr{C}$ of a deformable body is the set of deformation mappings which are globally one-to-one. In so-called *barrier* methods, the interpenetration constraint may be accounted for by adding the indicator function $I_{\mathscr{C}}(q)$ of the admissible set $\mathscr{C}$ to the energy of the solid. We recall that the indicator function of a set $\mathscr{C}$ is the extended-valued function

$$I_{\mathscr{C}}(q)=\begin{cases}0 & \text{if } q\in\mathscr{C}\\ \infty & \text{otherwise}\end{cases} \tag{75}$$

Often in calculations, the indicator function $I_{\mathscr{C}}$ is replaced by a penalty approximation $I_{\mathscr{C},\varepsilon}\geqslant 0$ parameterized by a small parameter $\varepsilon>0$ and such that $I_{\mathscr{C},\varepsilon}=0$ over $\mathscr{C}$. In this approach, as $\varepsilon\to 0$, $I_{\mathscr{C},\varepsilon}\to I_{\mathscr{C}}$ pointwise and interpenetration is increasingly penalized. A convenient choice of penalty energy function for contact with a rigid hyperplane is of the form

$$I_{\mathscr{C},\varepsilon}(q)=\frac{1}{2\varepsilon}\sum_{\alpha\in I}g_\alpha(q) \tag{76}$$

where the index set I ranges over all boundary nodes and

$$g_\alpha(q)=\begin{cases}0, & \text{if } (q-O)\cdot n\geqslant 0,\\ \|(q-O)\cdot n\|^2, & \text{otherwise,}\end{cases} \tag{77}$$

where O and n are the hyperplane reference point and outer-pointing normal. We note that the admissible set $I_{\mathscr{C},\varepsilon}$ is not invariant under the action of translations and rotations. It therefore follows that the constrained Lagrangian does not retain its momentum preserving properties and the Lagrangian reduction described in Section 4 cannot be carried out.

The application of force-stepping to dynamic contact problems is straightforward. The case in which the constraints are represented by means of a penalty energy function $I_{\mathscr{C},\varepsilon}$ falls right within the general framework and requires no special considerations, that is $V(q)=W(F(q))+I_{\mathscr{C},\varepsilon}(q)$. In addition, collision is automatically captured by the intrinsic time adaption of force-stepping (cf., e.g. [43, 44], for a detailed discussion of time-step selection considerations in contact problems).

Our example concerns the oblique impact of an elastic aluminum cube of size equal to 0.1 m. The mesh comprises 192 4-node tetrahedral isoparametric elements and 71 nodes. The cube is a compressible neo-Hookean solid characterized by a strain-energy density of the form (74). The values of the material constants in (74) are: $\lambda_0=60.5\,\mathrm{GPa}$, $\mu_0=26\,\mathrm{GPa}$, and $\rho=2700\,\mathrm{kg/m^3}$. The cube is imparted an initial velocity $v_0=(1,1,1)\,\mathrm{km/s}$. The rigid wall is described by a hyperplane with $O=(0.101, 0.101, 0.101)\,\mathrm{m}$ and $n=(0,-1,-1)$. A sequence of snapshots of the force-stepping trajectory corresponding to $h=5\cdot 10^{-4}\,\mathrm{m}$ are shown on Figures 19 and 20.

Figure 21 compares the time histories of the total energy, potential energy and kinetic energy attendant to the force-stepping trajectory for $h=5\times 10^{-4}\,\mathrm{m}$ and Newmark's trajectory for

DOI: 10.1002/nme

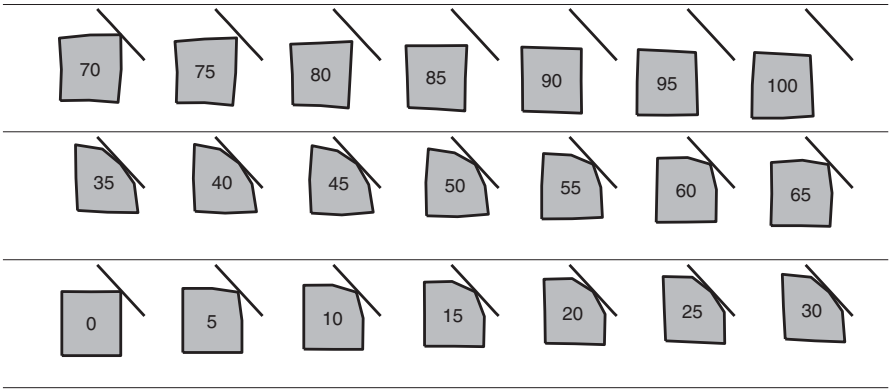

Figure 19. Oblique impact of neo-Hookean cube. Sequence of snapshots of the force-stepping trajectory with $h = 5 \times 10^{-4}$ m displaying the yz-midplane of the cube. Numbers indicate times in microsecond and oblique lines represent the rigid wall.

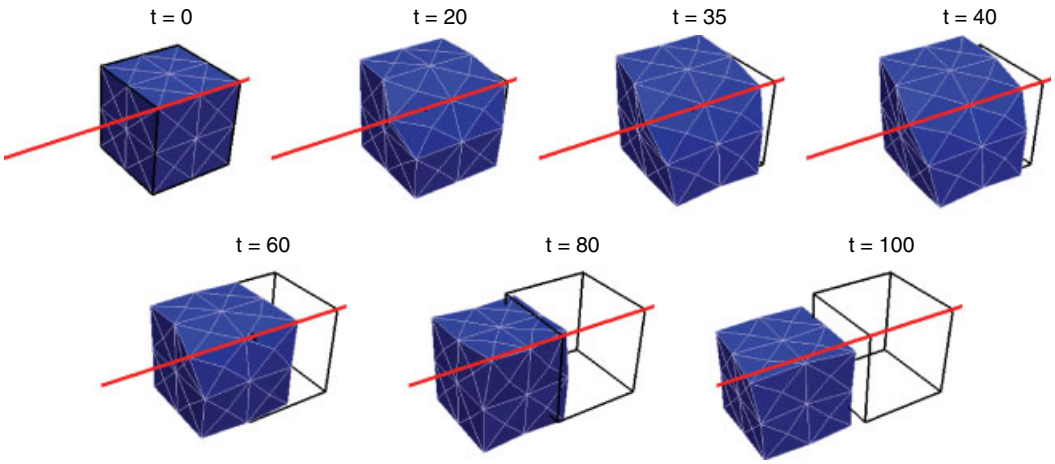

Figure 20. Oblique impact of neo-Hookean cube. Sequence of snapshots of the force-stepping trajectory with $h = 5 \times 10^{-4}$ m. Numbers indicate times in microsecond and lines provide a reference for the first points of impact, that is the $(x, 0.101, 0.101)$-line.

$\Delta t = 0.2$ ns, the latter chosen to be in the order of the average time step resulting from the force-stepping calculations. As expected, the kinetic energy of the system is partly converted to potential energy during the approach part of the collision sequence, and vice versa during the release part. Also characteristically, force-stepping is observed to conserve energy exactly through the collision, whereas the Newmark energy remains within tight bounds due to the small time step and the appropriate penalty energy, i.e. (76) and (77) with $\varepsilon = 10^{-14}$. Other notable features of the calculations are the ability of force-stepping to detect the time of collision and to automatically modulate the time-step so as to resolve the fine structure of the intricate interactions that occur through the collision.

DOI: 10.1002/nme

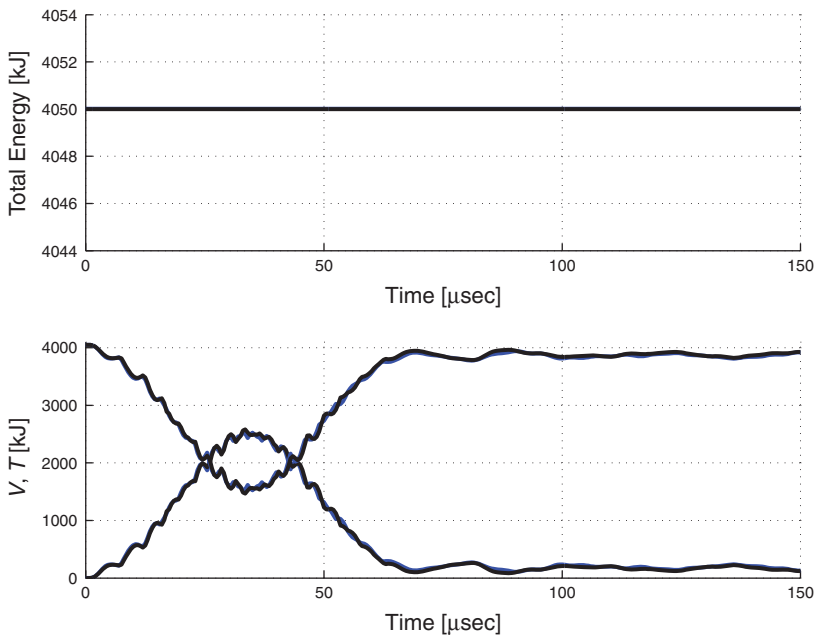

Figure 21. Oblique impact of neo-Hookean cube. Blue (or grey) line: Force-stepping solution with $h = 5 \times 10^{-4}$ m. Black line: Newmark solution with $\Delta t = 0.2$ ns.

Figure 22 shows the time history of the linear and angular momenta of the cube. Because the cube impacts with a rigid wall, the total linear and angular momenta of the system are not conserved through the collision but evolve in a characteristic way with time. We note from Figure 22 that the force-stepping trajectory does indeed follow closely Newmark's trajectory, although force-stepping does not conserve the linear and angular momenta. We also note that the transfer of linear momentum from the rigid wall to the cube is in the direction normal to the hyperplane and the motion in the orthogonal direction is unperturbed. Similarly, the oblique impact introduces angular momentum into the system. The good momentum behavior of force-stepping is noteworthy and may be understood as a consequence of the near-momentum conservation properties of the method (Theorem 4.2).

Finally, we investigate the relationship between the average time step and the number of degrees of freedom of the system $d = 3$N. To this end we consider three different meshes with increasing level of refinement, i.e. meshes I, II, and II with 213, 375, and 1287 degrees of freedom, respectively. Figure 23 shows the average time step selected by force-stepping is $O(h/N^2)$, where h is the simplicial grid size. We note that these results are consistent with and extend the results obtained in Section 6.2, i.e. a dependence of the form $O(h)$.

7. SUMMARY AND DISCUSSION

We have formulated a class of integration schemes for Lagrangian mechanics, which we refer to as *force-stepping integrators*, that are symplectic-energy and time-reversible with automatic

DOI: 10.1002/nme

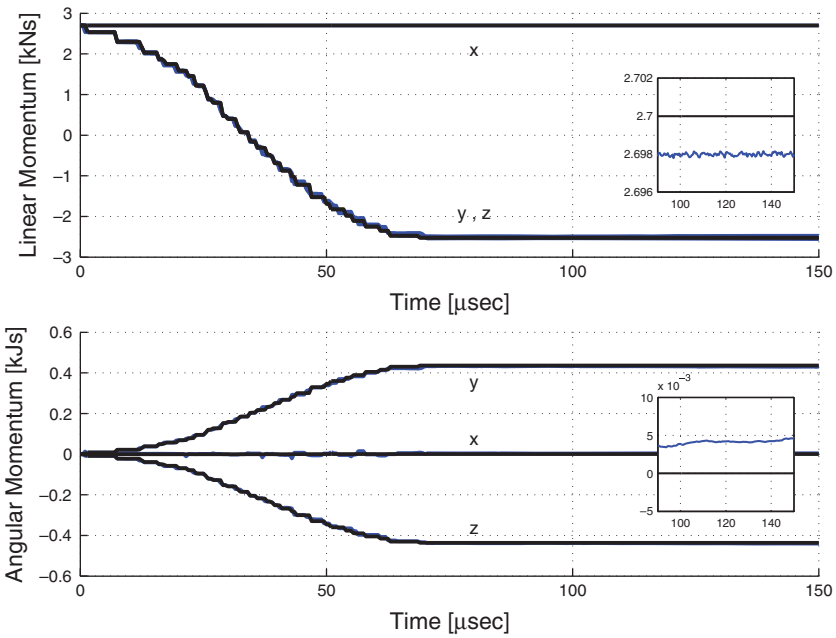

Figure 22. Oblique impact of neo-Hookean cube. Blue (or grey) line: Force-stepping solution with $h = 5 \times 10^{-4}$ m. Black line: Newmark solution with $\Delta t = 0.2$ ns. The insets show in detail the x-component of momentum maps.

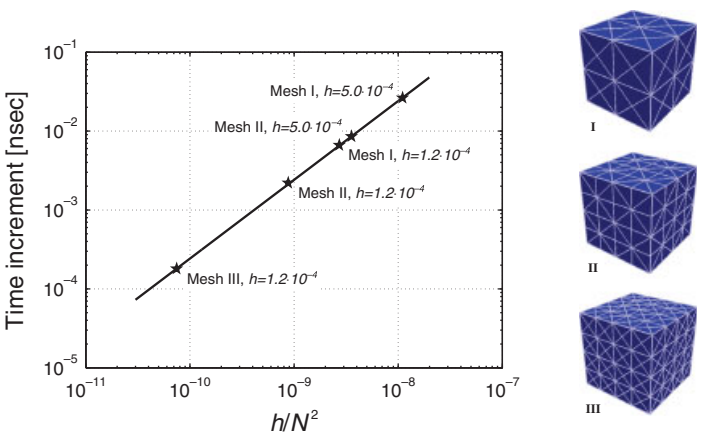

Figure 23. Oblique impact of neo-Hookean cube. The average time step selected by force-stepping is $O(h/N^2)$, where h is the simplicial grid size and $3N$ is the number of degrees of freedom of the system. Three different meshes are considered and depicted on the right-hand side.

DOI: 10.1002/nme

selection of the time-step size. The scheme also conserves approximately all the momentum maps associated with the symmetries of the system. Exact conservation of momentum maps may be achieved by recourse to Lagrangian reduction. The general strategy leading to the formulation of the force-stepping scheme, and its forerunner, the energy-stepping scheme [1], may be viewed as the reverse of backward-error analysis [45,46]. Thus, whereas backward-error analysis seeks to identify a nearby Lagrangian system that is solved exactly by the solutions generated by a numerical integrator, the approach followed here is to directly replace the system by a nearby one that can be solved exactly. The force-stepping scheme is obtained by replacing the original—or reduced—potential energy by a piecewise affine approximation over a simplicial grid, or regular triangulation. By taking triangulations of diminishing size, an approximating sequence of energies is generated. The trajectories of the resulting approximate Lagrangians can be characterized explicitly and consist of piecewise parabolic motion, or *free fall*. We have shown that the force-stepping trajectories are symplectic, energy preserving, approximately conserve momentum maps of the original system and, except for a negligible small set of initial conditions, converge to trajectories of the original system when the size of the simplicial grid is decreased to zero. Selected numerical tests, including the Kepler problem, the dynamics of a frozen argon cluster, and the oblique impact of an elastic cube, demonstrate the excellent long-term behavior of force-stepping, its automatic time-step selection property, and the ease with which it deals with constraints, including contact problems.

We have also described a unique, systematic and efficient representation of the piecewise-linear approximation of the potential based on a regular triangulation of $\mathbb{R}^d$ into proper simplices. The interpolation of the approximate potential can be restricted to one simplex at a time, and the *replacement rule* provides an efficient scheme to construct adjacent simplices as the numerical solution crosses simplicial boundaries. In particular, we have developed an algorithm for updating all simplex-related matrices required to compute force-stepping trajectories that has complexity $O(d^2)$.

We close by pointing out some limitations of our analysis and possible avenues for extensions of the approach.

First, our analysis of near conservation of momentum maps holds for given time intervals $[0, T]$ with $T < \infty$ that is the momentum map of force-stepping trajectories converges to the original one in $W^{1,\infty}_{\mathrm{loc}}([0, \infty))$. It is possible that such analysis can be extended to $W^{1,\infty}([0, \infty))$ if conditions under which approximating trajectory errors average out over long times are understood. Our experience with selected numerical tests suggests that the nearly-conserved momentum maps remain within tight bounds for long periods of time. However, a rigorous analysis of this property is beyond the scope of this paper.

Second, automatic time-step selection is an attractive feature of the force-stepping scheme. We have shown a linear relationship between the simplicial grid size and the average time step. In practice, this scaling could be improved by using triangulations that require fewer simplices. The review of Brandts *et al.* [47] on non-obtuse simplicial partitions, the work of Bliss and Su [48] on lower bounds for simplicial covers and triangulations of cubes, and other related work suggest possible directions in that regard.

Third, piecewise polynomial interpolation of the potential, including piecewise constant interpolation (*energy-stepping* [1]) and piecewise linear interpolation (*force-stepping*) do not exhaust the class of approximations that generate exactly solvable Lagrangians. A case in point concerns using discontinuous piecewise-linear approximations of the potential energy over a grid of polytopes. However, the criteria for constructing the piecewise-linear patches and convergence properties of the resulting time integrator are not well-understood at present. The systematic investigation

DOI: 10.1002/nme

of approximation schemes of the type proposed here, the elucidation of their properties and the determination of the best types of approximating Lagrangians in each area of application, are worthwhile directions of future research.

ACKNOWLEDGEMENTS

The authors gratefully acknowledge the support of the US Department of Energy through Caltech's PSAAP Center for the Predictive Modeling and Simulation of High-Energy Density Dynamic Response of Materials.

REFERENCES

1. Gonzalez M, Schmidt B, Ortiz M. Energy-stepping integrators in Lagrangian mechanics. *International Journal for Numerical Methods in Engineering* 2009; **82**(2):205–241.
2. Marsden JE, West M. Discrete mechanics and variational integrators. *Acta Numerica* 2001; **10**:357–514.
3. Lew A, Marsden JE, Ortiz M, West M. An overview of variational integrators. *Finite Element Methods*: *1970's and Beyond*. CIMNE: Barcelona, 2003.
4. Lew A, Marsden JE, Ortiz M, West M. Variational time integrators. *International Journal for Numerical Methods in Engineering* 2004; **60**(1):151–212.
5. Ge Z, Marsden JE. Lie–Poisson integrators and Lie–Poisson Hamilton–Jacobi theory. *Physics Letters A* 1988; **133**(3):134–139.
6. Katzenelson J. An algorithm for solving nonlinear networks. *Bell System Technical Journal* 1965; **44**:1605–1620.
7. Chien M-J, Kuh ES. Solving nonlinear resistive networks using piecewise-linear analysis and simplicial subdivision. *IEEE Transactions on Circuits and Systems* 1977; **24**(6):305–317.
8. Chua LO. Efficient computer algorithms for piecewise-linear analysis of resistive nonlinear networks. *IEEE Transactions on Circuits Theory* 1971; **18**(1):73–85.
9. Fujisawa T, Kuh ES. Piecewise-linear theory of nonlinear networks. *SIAM Journal on Applied Mathematics* 1972; **22**(2):307–328.
10. Chien M. Searching for multiple solutions of nonlinear systems. *IEEE Transactions on Circuits and Systems* 1979; **22**(10):817–827.
11. Kang S, Chua LO. A global representation of multidimensional piecewise-linear functions with linear partitions. *IEEE Transactions on Circuits and Systems* 1978; **25**(11):938–940.
12. Lin JN, Xu H, Unbehauen R. A generalization of canonical piecewise-linear functions. *IEEE Transactions on Circuits and Systems I* 1994; **41**(4):345–347.
13. Julián P, Desages A, Agamennoni O. High-level canonical piecewise-linear representation using a simplicial partition. *IEEE Transactions on Circuits and Systems I* 1999; **46**(4):463–480.
14. Kuhn HW. Some combinatorial lemmas in topology. *IBM Journal of Research and Development* 1960; **4**:518–524.
15. Hager WW. Updating the inverse of a matrix. *SIAM Review* 1989; **31**(2):221–239.
16. Marsden JE, Ratiu TS. *Introduction to Mechanics and Symmetry* (2nd edn). Springer: New York, 1999.
17. Marsden JE, Misiolek G, Ortega J-P, Perlmutter M, Ratiu TS. *Hamiltonian Reduction by Stages*. Springer: New York, 2007.
18. Meyer KR, Hall GR. *Introduction to Hamiltonian Dynamical Systems and the n-Body Problem*. Applied Mathematical Sciences, vol. 90. Springer: New York, 1992.
19. Littlejohn RG, Reinsch M. Internal or shape coordinates in the *n*-body problem. *Physical Review A* 1995; **52**(3):2035–2051.
20. Littlejohn RG, Reinsch M. Gauge fields in the separation of ratations and internal motions in the *n*-body problem. *Reviews of Modern Physics* 1997; **69**(1):213–275.
21. Pesonen J. Vibratio-rotation kinetic energy operators: a geometric algebra approach. *Journal of Chemical Physics* 2001; **114**(24):10598–10607.
22. Yanao T, Koon WS, Marsden JE. Gyration-radius dynamics in structural transitions of atomic clusters. *Journal of Chemical Physics* 2007; **126**:124102.
23. Hairer E, Lubich C, Wanner G, *Geometric Numerical Integration. Structure-Preserving Algorithms for Ordinary Differential Equations* (2nd edn). Springer Series in Computational Mathematics, vol. 31. Springer: Berlin, 2006.

DOI: 10.1002/nme

24. Arnold VI. *Mathematical Methods of Classical Mechanics* (2nd edn). Graduate Texts in Mathematics, vol. 60. Springer: New York, 1980.
25. Abraham R, Marsden JE. *Foundations of Mechanics* (2nd edn). Addison-Wesley: Redwood City, CA, 1987.
26. Hofer H, Zehnder E. *Symplectic Invariants and Hamiltonian Dynamics*. Birkhäuser Advanced Texts. Birkhäuser: Basel, 1994.
27. Whitney H. *Geometric Integration Theory*. Princeton University Press: Princeton, NJ, 1957.
28. Gol'dshtein V, Dubrovskiy S. Lemma Poincaré for $L_{\infty,loc}$-forms, 2007; arXiv:0712.1682v1. Available from: http://arxiv.org/abs/0712.1682.
29. McLachlan R, Scovel C. A survey of open problems in symplectic integration. *Fields Institute Communications* 1996; **10**:151–180.
30. Calvo MP, Sanz-Serna JM. The development of variable-step symplectic integrators, with applications to the two-body problem. *SIAM Journal on Scientific Computing* 1993; **4**:936–952.
31. Gladman B, Duncan M, Candy J. Symplectic integrators for long-term integrations in celestial mechanics. *Celestial Mechanics and Dynamical Astronomy* 1991; **52**:221–240.
32. Kane C, Marsden JE, Ortiz M, West M. Variational integrators and the Newmark algorithm for conservative and dissipative mechanical systems. *International Journal for Numerical Methods in Engineering* 2000; **49**(10): 1295–1325.
33. Belytschko T, Schoeberle D. On the unconditional stability of an implicit algorithm for nonlinear structural dynamics. *Journal of Applied Mechanics* 1975; **42**:865–869.
34. Hughes TJR. *The Finite Element Method*: *Linear Static and Dynamic Finite Element Analysis*. Prentice-Hall: Englewood Cliffs, NJ, 1997.
35. LaBudde RA, Greenspan D. Discrete mechanics—a general treatment. *Journal of Computational Physics* 1974; **15**:134–167.
36. Kane C, Marsden JE, Ortiz M. Symplectic energy-momentum integrators. *Journal of Mathematical Physics* 1999; **40**(7):3353–3371.
37. Lew A, Marsden JE, Ortiz M, West M. Asynchronous variational integrators. *Archive for Rational Mechanics and Analysis* 2003; **167**:85–146.
38. Bathe K-J. *Finite Element Procedures*. Prentice-Hall: Englewood Cliffs, NJ, 1996.
39. Zienkiewicz OC, Taylor RL. *The Finite Element Method* (5th edn). Butterworth-Heinemann: Stonehamm, MA, 2000.
40. Izaguirre JA, Reich S, Skeel RD. Longer time steps for molecular dynamics. *Journal of Chemical Physics* 1999; **110**(20):9853–9864.
41. Humphreys DD, Friesner RA, Berne BJ. A multiple-time step molecular dynamics algorithm for macromolecules. *Journal of Chemical Physics* 1994; **98**(27):6885–6892.
42. Biesiadecki JJ, Skeel RD. Dangers of multiple time step methods. *Journal of Computational Physics* 1993; **109**:318–328.
43. Carpenter NJ, Taylor RL, Katona MG. Lagrange constraints for transient finite-element surface-contact. *International Journal for Numerical Methods in Engineering* 1991; **32**(1):103–128.
44. Wriggers P. *Computational Contact Mechanics*. Wiley: New York, 2002.
45. Reich S. Backward error analysis for numerical integrators. *SIAM Journal on Numerical Analysis* 1999; **36**: 1549–1570.
46. Hairer E, Lubich C. The life-span of backward error analysis for numerical integrators. *Numerische Mathematik* 1997; **76**:441–462.
47. Brandts J, Korotov S, Křížek M, Šolc J. On nonobtuse simplicial partitions. *SIAM Review* 2009; **51**(2):317–335.
48. Bliss A, Su FE. Lower bounds for simplicial covers and triangulations of cubes. *Discrete and Computational Geometry* 2005; **33**:669–686.

DOI: 10.1002/nme